

001  
002  
003  
004  
005  
006  
007  
008  
009  
010  
011  
012  
013  
014  
015  
016  
017  
018  
019  
020  
021  
022  
023  
024  
025  
026  
027  
028  
029  
030  
031  
032  
033  
034  
035  
036  
037  
038  
039  
040  
041  
042  
043  
044  
045  
046

# Microbial symbionts buffer hosts from the demographic costs of environmental stochasticity

Joshua C. Fowler<sup>1,2\*</sup>, Shaun Ziegler<sup>3</sup>, Kenneth D. Whitney<sup>3</sup>,  
Jennifer A. Rudgers<sup>3</sup>, Tom E.X. Miller<sup>1</sup>

<sup>1</sup>\*Department of BioSciences, Rice University, Houston, 77005, TX, USA.  
<sup>2</sup>Department of Biology, University of Miami, Miami, 33146, FL, USA.  
<sup>3</sup>Department of Biology, University of New Mexico, Albuquerque, 87131, NM, USA.

\*Corresponding author(s). E-mail(s): [jcf221@miami.edu](mailto:jcf221@miami.edu);  
Contributing authors: [shaun.ziegler@gmail.com](mailto:shaun.ziegler@gmail.com); [whitneyk@unm.edu](mailto:whitneyk@unm.edu);  
[jrudgers@unm.edu](mailto:jrudgers@unm.edu); [tom.miller@rice.edu](mailto:tom.miller@rice.edu);  
Phone: 719-359-2960

#### Author Contributions

J.C.F. contributed to data collection, data analysis, and led manuscript drafting. S.Z. contributed to data collection and manuscript revisions. K.D.W. contributed to research conception, data collection, and manuscript revisions. J.A.R. established transplant plots, contributed to research conception, data collection, and manuscript revisions. T.E.X.M. contributed to research conception, data collection, data analysis, and manuscript revisions.

#### Data and Code Accessibility

Data will be made accessible as an Environmental Data Initiative package online DOI: [updated here when available](#). Code for all analysis is available through [add github repo](#)

**Article Type:** Letter

**Running Title:** Symbiont-mediated demographic buffering

**Keywords:** stochasticity, demography, symbiosis, mutualism, Epichloë

**This file contains:** Abstract ( XX words), Main Text (XX words), Figures (1-4); Supporting information Methods, Supporting Figures A1-A28, Supplemental Tables S1-S4

047  
048  
049  
050  
051  
052  
053  
054  
055  
056  
057  
058  
059  
060  
061  
062  
063  
064  
065  
066  
067  
068  
069  
070  
071  
072  
073  
074  
075  
076  
077  
078  
079  
080  
081  
082  
083  
084  
085  
086  
087  
088  
089  
090  
091  
092

### Abstract

Species' persistence in increasingly variable future climates will depend on resilience against the fitness costs of environmental stochasticity. Most organisms host microbiota that shield against stressors, and here, we show that, by limiting exposure to environmental extremes, microbial symbionts reduce hosts' demographic variance. We parameterized stochastic demographic models with a 14-year symbiont-removal experiment including seven host grasses of *Epichlē* fungal endophytes to demonstrate variance buffering as a novel pathway of host-symbiont mutualism. Symbionts reduced variance in fitness by > 10% on average across hosts, with up to 50% reductions for some host species. Hosts with "fast" life history traits that lacked longevity as an intrinsic buffer benefited most from symbiont-mediated buffering. Observed contributions of variance buffering were modest compared to symbiont benefits to mean fitness, which have dominated prior research. However, simulations of increased environmental stochasticity amplified benefits of variance buffering beyond symbionts' mean effects. Microbial-mediated variance buffering is likely an important, yet cryptic, mechanism of resilience in an increasingly variable world.

|  |     |
|--|-----|
| <b>Introduction</b>  | 093 |
| Global climate change involves increases in environmental variability, including changes to precipitation patterns and the frequency of extreme weather events [1, 2]. Yet, the ecological consequences of increased variability are less well understood than those of changing climate means, such as long-term warming or drying. Incorporating environmental variability into forecasts of population dynamics can improve predictions of the future.  | 094 |
| Classic theory predicts that long-term population growth rates (equivalently, population mean fitness) will decline under increased environmental stochasticity because the costs of bad years outweigh the benefits of good years – a consequence of nonlinear averaging [3, 4]. For example, in unstructured populations, the long-term stochastic growth rate in a fluctuating environment ( $\lambda_s$ ) will always be lower than the average growth rate ( $\bar{\lambda}$ ) by an amount proportional to the environmental variance ( $\sigma^2$ ):  | 095 |
| $\log(\lambda_s) \approx \log(\bar{\lambda}) - \frac{\sigma^2}{2\bar{\lambda}^2} \quad (1)$  | 096 |
| Populations structured by size or stage similarly experience costs of variability [5, 6]. There are accordingly two pathways to increase population viability in a variable environment: increase the mean growth rate and/or dampen temporal fluctuation in growth rates, also called “variance buffering”.   | 097 |
| Both the characteristics of species and the properties of their environment can buffer demographic fluctuations, including life history traits such as longevity [7, 8], correlations among vital rates [9], transient shifts in population structure [10], the magnitude of environmental variability [11], or the degree of environmental autocorrelation [12, 13]. These factors determine the risks of extinction faced by populations [14] and underlie management strategies promoting ecosystem resilience [15]. Yet little is known about how biotic interactions influence demographic variability or contribute to variance buffering [16].  | 098 |
| Most multicellular organisms host symbiotic microbes that affect growth and performance [17, 18], and many of these are transmitted via reproduction from maternal hosts to offspring [19]. This process of vertical transmission links the fitness of hosts and symbionts in a feedback loop that selects for mutual benefits [20]. Many vertically-transmitted microbes are mutualistic and protect hosts from stressful environmental conditions including drought, extreme temperatures, or natural enemies [21, 22]. Some of the best studied examples include bacterial symbionts of aphids and other insects that provide their hosts with thermal tolerance through the production of heat-shock proteins [23], and plant-fungal symbionts that produce anti-herbivore toxins [24–26]. However, these diverse protective symbioses are context-dependent: the magnitude of benefits depends on environmental conditions [27] and thus will vary temporally in a stochastic environment [28]. We hypothesized that context-dependent benefits from symbionts may buffer hosts against variability through strong benefits during harsh periods and neutral or even costly outcomes during benign periods, reducing the impacts of host exposure to extremes and dampening inter-annual variance relative to non-symbiotic hosts. Variance buffering is a previously unexplored mechanism by | 099 |
|  | 100 |
|  | 101 |
|  | 102 |
|  | 103 |
|  | 104 |
|  | 105 |
|  | 106 |
|  | 107 |
|  | 108 |
|  | 109 |
|  | 110 |
|  | 111 |
|  | 112 |
|  | 113 |
|  | 114 |
|  | 115 |
|  | 116 |
|  | 117 |
|  | 118 |
|  | 119 |
|  | 120 |
|  | 121 |
|  | 122 |
|  | 123 |
|  | 124 |
|  | 125 |
|  | 126 |
|  | 127 |
|  | 128 |
|  | 129 |
|  | 130 |
|  | 131 |
|  | 132 |
|  | 133 |
|  | 134 |
|  | 135 |
|  | 136 |
|  | 137 |
|  | 138 |

139 which symbionts may benefit their hosts instead of or in addition to elevating average  
140 fitness, the focus of most previous research.

141 We tested the hypothesis that context-dependent benefits of symbiosis buffer hosts  
142 from the fitness costs of environmental stochasticity. We used cool-season grasses and  
143 *Epichloë* fungal endophytes as a tractable experimental model in which non-symbiotic  
144 plants can be derived from naturally symbiotic plants through heat treatment, provid-  
145 ing a contrast of symbiont effects that controls for the confounding influence of host  
146 genetic background. *Epichloë* endophytes are specialized symbionts growing intercel-  
147 lularly in the aboveground tissue of ~ 30% of cool-season ( $C_3$ ) grass species [29].  
148 These fungi are primarily transmitted vertically from maternal plants through seeds  
149 [30]. They produce a variety of alkaloids that can protect host plants from herbivory  
150 [31] and drought stress [32].

151 Over 14 years (2007–2021), we collected annual demographic data on the survival,  
152 growth, reproduction, and recruitment of all plants within replicated endophyte-  
153 symbiotic and endophyte-free populations at our field site in southern Indiana, USA.  
154 Through taxonomic replication (seven host-symbiont species pairs) we aimed to under-  
155 stand whether host life history traits could explain inter-specific variation in the  
156 magnitude of demographic buffering through symbiosis. We used this long-term demo-  
157 graphic data to parameterize stochastic population projection models in a hierarchical  
158 Bayesian framework. Specifically, we (i) quantified the effect of symbiosis on the  
159 mean and variance of host vital rates (survival, growth and reproduction) and fit-  
160 ness, (ii) evaluated the relationship between host life history traits and the magnitude  
161 of symbiont-mediated variance buffering, (iii) determined the relative contribution of  
162 symbiont-mediated mean and variance effects to long-term population growth rates,  
163 and (iv) projected change in the magnitude of symbiont-mediated variance buffering  
164 under increased environmental variability of the future.  
165

## 166 Materials and Methods

### 167 Study site and species

168 This study was conducted at Indiana University's Lilly-Dickey Woods Research and  
169 Teaching Preserve (39.238533, -86.218150) in Brown County, Indiana, USA. This site  
170 is part of the Eastern broadleaf forests of southern Indiana, where the ranges of many  
171 understory cool-season grass species overlap. The experiment focused on seven of these  
172 grasses which host *Epichloë* endophytes (*Agrostis perennans*, *Elymus villosus*, *Ely-*  
173 *mus virginicus*, *Festuca subverticillata*, *Lolium arundinaceum*, *Poa alsodes*, and *Poa*  
174 *sylvestris*) (Table S1).  
175

### 176 Endophyte removal, plant propagation, and field set-up

177 Seeds from naturally symbiotic populations of the seven focal host species were col-  
178 lected during summer-fall 2006 from Lilly-Dickey Woods and the nearby Bayles Road  
179 Teaching and Research Preserve (39.220167, -86.542683). To generate symbiotic (S+)  
180 and symbiont-free (S-) plants from the same genetic lineages, seeds from each species  
181 were disinfected with a heat treatment described in Table S1 or left untreated. The heat  
182  
183  
184

treatment created symbiont-free plants by warming seeds to temperatures at which the fungus becomes inviable but the host seeds can still germinate. Both heat-treated and untreated seeds were surface sterilized with bleach to remove epiphyllous microbes, cold stratified for up to 4 weeks, then germinated in a growth chamber before transfer to the greenhouse at Indiana University where they grew for ~ 8 weeks. We confirmed endophyte status by staining thin sections of inner leaf sheath with aniline blue and examining tissue for fungal hyphae at 200X magnification [33]. We established experimental populations with vegetatively propagated clones of similar sizes. By starting the experiment with plants of similar sizes and the same number of unique genotypes, we aimed to limit any potential effects of heat treatments on initial plant growth [34].

During the fall of 2007 and spring of 2008, we established 10 3x3 m. plots for *A. perennans*, *E. villosus*, *E. virginicus*, *F. subverticillata*, and *L. arundinaceum* and 18 plots for *P. alsodes* and *P. sylvestris*. Half of the plots were randomly assigned to be planted with either symbiotic or with symbiont-free plants, and initiated with 20 evenly spaced individuals labeled with aluminum tags. In spring 2008, we placed plastic deer net fencing around each plot to limit deer herbivory and disturbance; damaged fences were regularly replaced.

### Long-term demographic data collection

Each summer starting in 2008 through 2021, we censused all individuals in each plot for survival, growth and reproduction, adding new recruits to the census. Plots contained 13.3 individuals/m<sup>2</sup> on average over the course of the experiment. Each census year was a sample of inter-annual climatic variation (n = 14 years; comprising 13 demographic transition years). We censused each species during its peak fruiting stage (May: *Poa alsodes*, *Poa sylvestris*; June: *Festuca subverticillata*; July: *Elymus villosus*, *Elymus virginicus*, *Lolium arundinaceum*; September: *Agrostis perennans*), such that the censuses were pre-breeding and new recruits came from the previous years' seed production. Leaf litter was cleared out of each plot prior to the census, to aid in locating plants. For each plant remaining from the previous year, we determined survival, measured its size as a count of tillers, and collected reproductive data as counts of reproductive tillers and seed-bearing spikelets on all reproductive tillers to a maximum of three. We also tagged all unmarked individuals that were recruits from the previous years' seed production and collected the same demographic data. New recruits typically had one tiller and were non-reproductive. In 2008 and 2009, we took additional counts of seeds per inflorescence for all reproducing individuals in the plots to ground-truth our sub-sample estimates. For *Agrostis perennans*, we also collected seed counts in 2010. In 2018, we stopped collecting data for the *Lolium arundinaceum* plots, which had very high survival and low recruitment, and consequently very low variation across years. For each individual in the experiment, our data recorded their transitions in size and reproduction from one year to the next. In total across 14 years, the dataset included demographic information for 16,789 individual host-plants and 31,216 transition-year observations.

We expected plots to maintain their endophyte status (symbiotic or symbiont-free) because the fungal symbionts are almost exclusively vertically transmitted, and plots

231 were spaced a minimum of 5 m apart, limiting seed dispersal or horizontal trans-  
 232 mission of the symbiont between plots. However, we regularly confirmed endophyte  
 233 treatment throughout the lifetime of the experiment by opportunistically taking sub-  
 234 sets of seeds from reproductive individuals and scoring them for their endophyte status  
 235 with microscopy as above. Overall, these scores reflected 98% faithfulness of recruits  
 236 to their expected endophyte status across species and plots (Fig. S23; Supplement  
 237 data). Additionally, we have rarely observed fungal stromata, the fruiting bodies by  
 238 which *Epichloë* are potentially transmitted horizontally, provided the fly vector is also  
 239 present [35]. For *A. perennans*, *F. subverticillata*, *L. arundinaceum*, and *P. alsodes*, we  
 240 never observed stromata. We observed stromata only infrequently for *E. villosus*, and  
 241 even more rarely for *E. virginicus* and *P. sylvestris* (Table S2). For these species, stro-  
 242 mata have only been observed on 35, 4, and 6 plants respectively, making up < 0.3% of  
 243 all censused plants (Supplemental data). These stromata observations occurred irreg-  
 244 ularly across years; in most years there were no stromata during the census, and in a  
 245 few years several plants produced stromata.  
 246

## 247 Vital rate modeling

248 Equipped with these demographic data, we fit statistical models for survival, growth,  
 249 flowering (yes or no), fertility of flowering plants (number of flowering tillers), produc-  
 250 tion of seed-bearing spikelets (number per inflorescence), the average number of seeds  
 251 per spikelet, and the recruitment of seedlings from the preceding year's seed produc-  
 252 tion (Fig. S1 - S10). We fit these vital rates as generalized linear mixed models in a  
 253 hierarchical Bayesian framework using RStan [36] which allowed us to isolate endo-  
 254 phyte effects on vital rate means and variances, borrow strength across species for  
 255 some variance components, and propagate uncertainty from the individual-level vital  
 256 rates to population projection models [37]. All vital rate models included random plot  
 257 and year effects, with separate estimates of year-to-year variance for symbiotic and  
 258 symbiont-free plants, to quantify the effect of endophytes on inter-annual variance  
 259 (Fig. S11 - S18). These variance components and other predictors as described below  
 260 were given vague priors [38]. We ran each vital rate model for 2500 warm-up and  
 261 2500 MCMC sampling iterations with three chains. We assessed model convergence  
 262 with trace plots of posterior chains and checked for  $\hat{R}$  values less than 1.01, indicat-  
 263 ing low within- and between-chain variation [39, 40]. For those models that showed  
 264 poor convergence, we extended the MCMC sampling to include 5000 warm-up and  
 265 5000 sampling iterations, which was only necessary for seedling growth. We graphi-  
 266 cally checked vital rate model fit with posterior predictive checks comparing simulated  
 267 data from 500 posterior draws with the observed data (Fig. S19-S20).

268 *Survival* - We modeled survival as a Bernoulli process, where the survival ( $S$ ) of  
 269 an individual  $i$  in plot  $p$  and census year  $t$  was predicted by the plot-level endophyte  
 270 status ( $e$ ), host species ( $h$ ), size in the preceding census, and the plant's origin status  
 271 (whether it was initially transplanted or naturally recruited into the plot).

273  
 274  
 275  
 276

$$S_{i,p(e),h,t} \sim \text{Bernoulli}(\hat{S}_{i,p(e),h,t}) \quad (2a)$$

$$\begin{aligned} \text{logit}(\hat{S}_{i,p(e),h,t}) &= \beta_{0_h} + \beta_1 * \text{origin}_i & (2b) & 277 \\ &+ \beta_{2_h} * \text{endo}_i + \beta_{3_h} * \text{size}_{i,t-1} + \tau_{e,h,t} + \rho_p & (2c) & 278 \\ &\tau_{e,h,t} \sim \text{Normal}(0, \sigma_{\tau_{e,h}}^2) & (2d) & 279 \\ &\rho_p \sim \text{Normal}(0, \sigma_\rho^2) & (2e) & 280 \end{aligned}$$

Here,  $\hat{S}$  is the survival probability ( $p(e)$  indicates that plot identity is uniquely associated with an endophyte status),  $\beta_{0_h}$  is an intercept specific to each host species,  $\beta_1$  is the effect of the plant's recruitment origin,  $\beta_{2_h}$  is the endophyte effect,  $\beta_{3_h}$  is the size effect,  $\tau_{e,h,t}$  is a normally distributed year effect for each species and endophyte status with variance  $\sigma_{\tau_{e,h}}^2$ , and  $\rho_p$  is a normally distributed plot effect with variance  $\sigma_\rho^2$ . We assume that origin effect  $\beta_1$  and plot-to-plot variance  $\sigma_\rho^2$  are shared across host species, allowing us to "borrow strength" across the multi-species dataset; other model parameters are unique to host species. We separately modeled the survival of newly recruited seedlings, which were typically one tiller and non-reproductive, with a similar model but omitting size dependence and the effect of the plant's origin status. All random effects were estimated independently between seedling and adult vital rates models.

*Growth* - We modeled plant size in census year  $t$  ( $G$ ) with the same linear predictor for the mean as described for survival. Because we measured size as positive integer-valued counts of tillers, we modeled it with a zero-truncated Poisson-inverse Gaussian distribution. This distribution includes a shape parameter  $\lambda_G$  to account for overdispersion in the data. We additionally modeled the growth of newly recruited seedlings separately with a Poisson-inverse Gaussian model omitting size structure and the plants' origin status as with seedling survival.

*Flowering* - We modeled whether or not a plant was flowering during the census ( $P$ ) as a Bernoulli process, with the same linear predictor for the mean as described above for survival except that size dependence for reproductive vital rates was determined by the individual's size during the same census year as opposed to its size during the previous year.

*Fertility* - For a plant that was flowering during the census, its fertility was the number of reproductive tillers produced ( $F$ ), which we modeled as a function of size in the same census period with a zero-truncated Poisson-Inverse Gaussian distribution, with the same linear predictor for the mean as described above.

*Spikelets per Inflorescence* - Spikelet production ( $K$ ) was recorded as integer counts on up to three inflorescences per reproducing plant. We modeled these data with a negative binomial distribution, with the same linear predictor for the mean as described above.

*Seed Production per Spikelet* - For individuals with recorded counts of seed production, we calculated the number of seeds per spikelet from our counts of seeds and spikelets per inflorescence, and then modeled seeds per spikelet ( $D$ ) as means of a Gaussian distribution for each species and endophyte status. Because we had less detailed data across years and plants for seed production than for other reproductive vital rates, we omitted both plot and year random effects.

323     *Seedling Recruitment* - We used a binomial distribution to model the recruitment of  
 324 new seedlings ( $R$ ) into the plots from seeds produced in the preceding year, assuming  
 325 no long-lived seed bank. We included an intercept specific to each host and endophyte  
 326 status and the same random effects structure as in other models. We estimated the  
 327 number of seeds per plot in the preceding year by multiplying the total number of  
 328 reproductive tillers per plant by the mean number of spikelets per inflorescence on that  
 329 plant and by a sample from the posterior distribution of mean number of seeds per  
 330 spikelet ( $D$ ). For plants with missing fertility or spikelet data, we used the expected  
 331 number of reproductive tillers ( $F$ ) or of spikelets per inflorescence from ( $K$ ), drawing  
 332 from the full posteriors of our models. We rounded this value to get the estimated seed  
 333 production for each individual, and finally summed across all reproductive plants in  
 334 each year and plot to get the total number of seeds produced.  
 335

### 336 Stochastic population model

337 Using the fitted vital rate models, we parameterized stochastic matrix projection mod-  
 338 els including two state variables:  $r_t$  (the number of newly recruited individuals in year  
 339  $t$ ), and  $\mathbf{n}_t$  (a vector including all non-seedling individuals of sizes  $x \in \{1, 2, \dots, U\}$ , rang-  
 340 ing from one to the maximum number of tillers  $U$ . We used the same model structure  
 341 for each species and endophyte status (not shown in model notation, to make it more  
 342 readable). The total number of recruits in year  $t + 1$  is given by:  
 343

$$344 \quad r_{t+1} = \sum_{x=1}^U P(x; \boldsymbol{\tau}_P) F(x; \boldsymbol{\tau}_F) K(x; \boldsymbol{\tau}_K) D R(\boldsymbol{\tau}_R) n_t^x \quad (3)$$

345 The total number of seeds produced by a maternal plant of size  $x$  is the product  
 346 of the size-specific probability of flowering  $P$ , the number of reproductive tillers  $F$ ,  
 347 the number of spikelets per inflorescence  $K$ , and the number of seeds per spikelet  $D$ .  
 348 Multiplying by the probability of transitioning from seed to seedling  $R$  gives a per-  
 349 capita rate of seedling production, which is multiplied by the number of plants of  
 350 size  $x$  ( $n_t^x$ , the  $x^{\text{th}}$  element of  $n_t$ ) and summed. Each function also depends on the  
 351 species- and endophyte-specific year random effects for that vital rate ( $\boldsymbol{\tau}$ , a vector of  
 352 year-specific values derived from the statistical models).

353     Recruitment, survival and growth determine the rest of the population dynamics  
 354 of the new seedlings and larger plants. The number of  $y$ -sized plants in year  $t + 1$  is  
 355 given by:  
 356

$$357 \quad n_{t+1}^y = Z(y; \boldsymbol{\tau}_Z) B(\boldsymbol{\tau}_B) r_t + \sum_{x=1}^U S(x; \boldsymbol{\tau}_S) G(x, y; \boldsymbol{\tau}_G) n_t^x \quad (4)$$

358 where  $n_{t+1}^y$  is the  $y^{\text{th}}$  element of vector  $n_{t+1}$ . The first term on the right hand  
 359 side of Eqn. 4 represents growth ( $Z$ ) and survival ( $B$ ) of seedling recruits. The second  
 360 term includes the survival of  $x$ -sized plants and the growth of survivors from size  $x$   
 361 to  $y$ , summed over all  $x$ . To avoid predictions of unrealistic growth outside of the  
 362 observed size distribution, we set a ceiling on the growth function for plants at the  
 363 97.5<sup>th</sup> percentile in the observed size distribution [41].

364     Each of the functions in Eqns. 3 and 4 have separate intercepts and year random  
 365 effects for symbiotic and symbiont-free populations, allowing us to calculate the effect  
 366

of endophyte symbiosis on the mean and variance of  $\lambda$ , the dominant eigenvalue of the projection matrix. Analysis of climate-explicit population models followed the same logic as for the climate-implicit models presented here with the addition of parameters defining the relationship between either annual or growing season drought index and each vital rate. A full description of climate-explicit methods can be found in the Supporting Information Text.

## Life History Analysis

We collected metrics describing each host species' life history to test the relationship between pace of life and variance buffering (Table S1). Using the *Rage* package [42], we calculated  $R_0$ , longevity, and generation time from our estimated transition matrices using the symbiont-free mean matrix as the reference condition. We recorded seed size as the average lemma length from the Flora of North America [43]. We also calculated the 99th percentile of maximum observed age for each species from their S-populations. Next, we fit Bayesian phylogenetic mixed-effects models using the 'brms' package [44] to test the relationship between each life history trait and the estimated effect of symbiosis on the coefficient of variation from the population model while controlling for phylogenetic non-independence in the hosts (Fig. 26) and the symbiont (Fig. S27). We pruned larger species-level phylogenies of plants[45] and *Epichloë* fungi [46] to include the focal species. *Agrostis perennans* was not included in the tree, and so we used a congeneric species, *A. hyemalis*. We defined separate phylogenetic covariance matrices for each pruned tree. We propagated uncertainty in the estimated variance buffering effect with a measurement error model. Thus the model for the variance buffering effect  $V$  was given by:

$$\begin{aligned}
 V_{MEAN,h} &\sim Normal(V_{EST,h}, V_{SD,h}) & (5a) \\
 V_{EST,h} &\sim Normal(\mu_h, \sigma) & (5b) \\
 \mu &= \alpha + \beta * trait + \pi & (5c) \\
 \alpha &\sim Normal(0, .5) & (5d) \\
 \beta &\sim Normal(0, .1) & (5e) \\
 \sigma &\sim Half - Normal(.04, .01) & (5f) \\
 \pi &\sim Normal(0, \sigma_\pi * \mathbf{A}) & (5g) \\
 \sigma_\pi &\sim Half - Normal(0, .1) & (5h)
 \end{aligned}$$

Here,  $V_{EST}$  is the variance buffering effect for each host species  $h$ , estimated from the posterior mean ( $V_{MEAN}$ ) and standard deviation ( $V_{SD}$ ), propagating uncertainty associated with the effect of symbiosis in our population model. The model includes an intercept parameter ( $\alpha$ ) and a slope parameter ( $\beta$ ) defining the relationship between the variance buffering effect and the life history trait. The residual standard deviation is given by ( $\sigma$ ). We used weakly informative priors to aid model convergence. Each prior was centered at zero, except for the residual standard deviation, which we centered at the standard deviation of the estimated variance buffering effect, .04. The phylogenetic

415 random effect ( $\pi$ ) has a standard deviation ( $\sigma_\pi$ ) which is structured by the covariance  
416 matrix  $\mathbf{A}$ . We ran each MCMC sampling chain for 8000 warmup iterations and 2000  
417 sampling iterations. We assessed model convergence as described for the vital rate  
418 models.

419

## 420 Mean-variance decomposition

421

422 To calculate stochastic population growth rates ( $\lambda_s$ ) for each host species and endo-  
423 phyte status we simulated population dynamics for 1000 years by randomly sampling  
424 from the 13 annual transition matrices observed over the course of the experiment,  
425 discarding the first 100 years to minimize the influence of initial conditions. Sampling  
426 observed transition matrices produces models which realistically capture inter-annual  
427 variation by preserving correlations between vital rates [47]. We tallied the total pop-  
428 ulation size at each time step as  $N_t = r_t + \sum_{x=1}^U n_t^x$  and calculated the stochastic  
429 growth rate as  $\log(\lambda_s) = E[\log(\frac{N_t}{N_{t+1}})]$  [48, 49]. We calculated the total effect of endo-  
430 phyte symbiosis as the difference in  $\lambda_s$  between S+ and S- populations. We propagated  
431 uncertainty from the vital rate models to the calculation of  $\lambda_s$  using 500 draws from  
432 the posterior distribution of model parameters.

433 We decomposed the total endophyte effect on  $\lambda_s$  into contributions from effects  
434 on vital rate means, variances, and their interaction. Specifically, we repeated the  
435 calculation of  $\lambda_s$  for two additional “treatments”: (1) endophyte effects on mean vital  
436 rates only, with inter-annual variances shared between S+ and S- at the S- reference  
437 level for all vital rates, and (2) endophyte effects on vital rate variances only, with  
438 vital rate means shared between S+ and S- at the S- reference level. The combination  
439 of all four  $\lambda_s$  treatments (S+ vital rate means and variances, S- means and variances,  
440 S+ means with S- variances, S- means with S+ variances) allowed us to quantify to  
441 what extent the overall effect of symbiosis derives from changes in vital rates means,  
442 variances, and their interaction. The interaction occurs because the variance penalty to  
443 stochastic growth is proportional to the mean value of annual growth rates (see Eq. 1)  
444 such that variance is more detrimental for populations with low average growth rates.  
445 For each contribution element (variance buffering, mean effects, and their interaction),  
446 we calculated a cross-species mean to assess the overall contributions (Fig. 4).

447

## 448 Simulation experiment

449

450 To create scenarios of increased variance relative to that observed during the study  
451 period, we repeated the stochastic growth rate estimation and decomposition, but  
452 sampling only a subset of the 13 observed annual transition matrices. We created  
453 two scenarios of increased environmental variance by sampling the transition matrices  
454 associated with the six or two most extreme  $\lambda$  values, representing the six or two  
455 best and worst years, using S- populations as the reference condition. By sampling  
456 away from an average year in both directions, the mean value of annual growth rates  
457 remained similar across treatments ( $\bar{\lambda}$  averaged across species: All years = 0.71; 6  
458 years = 0.71; 2 years = 0.73; Fig. S21A), while the standard deviation more than  
459 doubled ( $sd(\lambda)$  averaged across species: All years = 0.25; 6 years = 0.34; 2 years =  
460 0.54 ; Fig. S21B), representing elevated environmental fluctuations. We performed the

same mean-variance decomposition for these scenarios as for the ambient conditions  
(all 13 years sampled) for all host species described above (Fig. S22). 461  
462  
463

## Results and Discussion 464

### Symbionts buffer host demographic variance 465

Across seven host species, eight vital rates, 14 years, and 16,789 individual plants, our 466  
analysis provided the first empirical evidence of symbiont-mediated variance buffering. 467  
Endophytes reduced inter-annual variance for 66% (37/56) of host species-vital rate 468  
combinations (average Cohen's D for effects on vital rate standard deviation: -0.15) 469  
(Fig 1A). Endophytes also increased mean vital rates for the majority (36/56) of host 470  
species-vital rate combinations (average Cohen's D for effects on vital rate mean: 0.15), 471  
and benefits were particularly strong for host survival, plant growth and recruitment 472  
(Fig. 1A). The relative magnitude of means and variances effects differed among host 473  
species and their vital rates. For example, endophytes modestly increased mean adult 474  
survival (Fig. 1C) and reduced variance in survival (Fig. 1D) for *Festuca subverticillata*, 475  
while for *Poa alsodes*, variance buffering was more apparent in seedling growth 476  
and inflorescence production (Fig 1E). Interestingly, certain vital rates showed costs 477  
of endophyte symbiosis. Symbiotic individuals of *A. perennans* grew larger than those 478  
without endophytes (Fig. 1B), yet endophytes also reduced this species' mean recruit- 479  
ment rates (Fig. 1A). In addition, endophyte symbiosis increased variance in seedling 480  
growth, rather than reducing variance, for *Elymus villosus* and *Festuca subverticillata* 481  
(Fig. 1A). 482  
483  
484  
485  
486  
487  
488  
489  
490  
491  
492  
493  
494  
495  
496  
497  
498  
499  
500  
501  
502  
503  
504  
505  
506

Because not all vital rates contribute equally to fitness, we used stochastic matrix 485  
models to integrate the diverse effects on vital rates described above into comprehensive 486  
measures for the mean and variance of year-to-year fitness ( $\lambda_t$ ) and the long-run 487  
fitness that integrates both mean and variance ( $\lambda_S$ ). On average across host species, 488  
endophyte-symbiotic populations had greater mean fitness (> 92% confidence that 489  
endophytes increased  $\bar{\lambda}$ ) and lower inter-annual variability in fitness (> 86% confidence 490  
that endophytes decreased the coefficient of variation of  $\lambda_t$ ) than endophyte-free 491  
populations (Fig. 2). For some host species, the CV of  $\lambda_t$  declined by as much as 170% 492  
(*P. alsodes*, *F. subverticillata*), while for others, endophyte effects on variance were 493  
substantially smaller (6% lower for *E. villosus*, 16% lower for *A. perennans*), or even 494  
positive (27% increase for *E. virginicus*). When mean and variance effects of sym- 495  
bionts were considered together, none of the host-symbiont pairings were antagonistic 496  
(i.e., with endophytes that both decreased mean fitness and increased variance) (Fig. 497  
2C), suggesting that variation across host species and vital rates in mean and variance 498  
effects may reflect alternative strategies that yield similar net benefits of endophyte 499  
symbiosis. 500  
501  
502  
503  
504  
505  
506

507 Precipitation-Evapotranspiration Index [50]) than symbiont-free populations (Sup-  
508 porting Information Text; Fig. S24-S25; Table S3). However, we did not find a strong  
509 relationship between the magnitude of variance buffering and relative drought sensi-  
510 tivities, suggesting that other climatic factors or other temporally-varying aspects of  
511 the biotic or abiotic environment may elicit benefits of endophyte symbiosis, including  
512 documented resistance to herbivory for six host taxa [51, 52].

513

#### 514 **Faster life histories predict stronger symbiont-mediated 515 variance buffering**

516

517 Theory predicts that long-lived species, those on the slow end of the slow-fast life  
518 history continuum, will be less sensitive to environmental variability than short-lived  
519 species [53], a pattern which has empirical support across plants [54] and animals  
520 [8, 55]. Therefore, host species with long lifespans that produce few, large offspring  
521 should benefit less from symbiont-mediated variance buffering than species with fast  
522 life cycles that produce many smaller offspring with low per-capita chance of success  
523 [56, 57]. In support of this prediction, hosts with trait values representing faster life  
524 history strategies experienced greater variance buffering from endophytes than those  
525 with slow life histories (Fig. 3). Bayesian phylogenetic mixed-effects models, controlling  
526 for species' relatedness, indicated that variance buffering was stronger for host species  
527 with shorter lifespan (Fig. 3A; 75% probability of positive relationship with empirically  
528 observed maximum plant age) and smaller seeds (Fig. 3B; 73% probability of positive  
529 relationship with seed length). Other life history traits similarly had positive, but  
530 weaker, support for the prediction that faster life history traits correlate with stronger  
531 variance buffering (Fig. S26-S28). Considering fungal life history traits, the three host  
532 species for which the net mutualism benefit was weakest (*Elymus villosus*, *Elymus*  
533 *virginicus*, and *Poa sylvestris*) (Fig. 2C) were the only hosts for which we observed  
534 fungal stromata, fruiting bodies capable of horizontal (contagious) transmission (Table  
535 S2). This result supports the theoretical expectation that strict vertical transmission  
536 drives the evolution of strong host-symbiont mutualism [20, 58]. Conclusions about  
537 life histories are somewhat constrained by the narrow range of trait values among  
538 closely related species in the grass sub-family Pooideae and their co-evolving symbionts.  
539 Our understanding of how life history variation modulates the fitness consequences of  
540 microbial symbiosis would profit from tests across a wider span of taxonomic groups  
541 [59].

542

#### 543 **Contributions from variance buffering are weak relative to 544 mean effects**

545

546 To evaluate the relative importance of mean fitness benefits and variance buffering as  
547 alternative pathways of mutualism, we decomposed the overall effect of the symbiosis  
548 on the stochastic growth rate  $\lambda_S$  using simulations from the population models in four  
549 configurations. The configurations included either the full symbiosis effect (both mean  
550 and variance buffering effects), mean effects alone, variance effects alone, or neither  
551 mean nor variance effects. Overall, the full effect of symbiosis on  $\lambda_S$ , averaged across  
552 host species, provided strong evidence of grass-endophyte mutualism (99% certainty

of a positive total effect on  $\lambda_s$ ) (Fig. 4; see Fig. S22 for individual host species).  
The full effect of symbiosis on  $\lambda_S$  was positive for seven out of eight species, with  
statistical confidence ranging from 66% to greater than 99% certainty, except for *P.*  
*sylvestris* which had only a 45% posterior probability of a positive full effect size (Fig  
S22). Contributions to this full effect derived from both mean and variance buffering  
effects, as well as a slightly negative interaction (i.e., the combined influence of mean  
and variance effects was smaller than the sum of their individual effects). Endophytes'  
contributions to  $\lambda_S$  from mean effects were four times greater, averaged across species,  
than contributions from variance buffering (Fig. 4), suggesting that, under the regime  
of environmental variability represented by our 14-year study, damped fluctuations  
in fitness via variance buffering was a far less important element of the benefits of  
symbiosis than increased mean fitness.

## Variance buffering strengthens under increased environmental variability

Simulations of increased environmental variability, a key prediction of climate change  
forecasts [2], indicated that mutualism with microbial symbionts, and their variance  
buffering effects in particular, will take on increased importance for hosts in a more  
variable future climate. To simulate increased variability, we repeated the decomposi-  
tion of  $\lambda_S$  for two alternative forecast scenarios, randomly sampling transition matrices  
that represented either the six most extreme years experienced by each species or  
the two most extreme years, subsets of the thirteen transition matrices across the  
14-year study period. The six- and two- years scenarios increased the standard devia-  
tion of yearly host growth rates by 1.3 and 2.1 times, respectively, without changing  
mean growth rates (< 2.3% difference in  $\bar{\lambda}$  between simulation treatments, Fig. S21).  
Increased variability elicited stronger mutualistic benefits of endophyte symbiosis (Fig.  
3) than ambient variability (overall effect of the symbiosis increased by > 130%). This  
increase was driven by increased contributions from the variance buffering mechanism  
(from a 24% contribution in the ambient scenario to a 66% contribution in the most  
variable scenario) rather than from greater mean effects. In the most variable scenario,  
the relative importance of mean and variance effects reversed, with variance buffering  
contributions that were 1.5 times greater than contributions from mean benefits, aver-  
aged across species (Fig. 4). Thus, variance buffering – a cryptic microbial influence  
that manifests only over long time scales – is poised to become the dominant way in  
which grasses benefit from symbiosis with fungal endophytes in more variable climates  
of the future.

Ecologists increasingly recognize the importance of symbiotic microbes for host  
organisms and the populations, communities, and ecosystems in which their hosts  
reside [60–63]. Despite awareness of these ubiquitous interactions, long-term stud-  
ies of microbial symbiosis are very rare. Our analysis of taxonomically-replicated,  
long-term field experiments that manipulated the presence/absence of fungal sym-  
bionts in plants demonstrates for the first time that heritable microbes can commonly  
benefit hosts not only through improved mean fitness – the focus of most previous  
research – but also through buffering against environmental variance. Our results  
provide an important advance to improve forecasts of the responses of populations

599 (and symbiota) to increasing environmental stochasticity under global change, sug-  
600 gesting that, for some host species, microbial symbiosis may compensate for the lack  
601 of intrinsic tolerance of variability conferred by “slow” life history traits. We found  
602 that symbiont-mediated variance buffering made relatively weak contributions to host-  
603 symbiont mutualism under the current regime of environmental variability, but is  
604 likely to become the dominant benefit that fungal endophytes confer to grass hosts in  
605 more variable future environments. This result emerges from the context-dependent  
606 nature of grass-endophyte interactions, combined with the observation that environ-  
607 mental stochasticity generates fluctuation in context. These key ingredients, and thus  
608 the potential for symbiont-mediated variance buffering, similarly apply to the diverse  
609 host-microbe symbioses across the tree of life.

610

611

612

613

614

615

616

617

618

619

620

621

622

623

624

625

626

627

628

629

630

631

632

633

634

635

636

637

638

639

640

641

642

643

644

|  |  |
|--|--|
| <b>Acknowledgments.</b> We thank Mark Sheehan, Ali Campbell, Kyle Dickens, Blaise Willis, and Sar Lindner for contributions to field data collection. We also thank Volker Rudolf, Daniel Kowal, Lydia Beaudrot and Judie Bronstein for helpful comments on and discussion of this project. This research was supported by the National Science Foundation (grants 1754468 and 2208857). | 645<br>646<br>647<br>648<br>649<br>650<br>651<br>652<br>653<br>654<br>655<br>656<br>657<br>658<br>659<br>660<br>661<br>662<br>663<br>664<br>665<br>666<br>667<br>668<br>669<br>670<br>671<br>672<br>673<br>674<br>675<br>676<br>677<br>678<br>679<br>680<br>681<br>682<br>683<br>684<br>685<br>686<br>687<br>688<br>689<br>690 |
| <b>Supplementary information.</b> Supplementary information for this paper includes Supplementary Methods, Figs. A1 to A28, and Tables A1 to A3.   |  |

691 **Supplemental Methods**

692 **Estimating climate drivers of environmental context-dependence**

694 To connect the variance buffering effects of endophytes with inter-annual variability  
695 in climate, we built climate-explicit stochastic matrix population models from the  
696 vital rate data in addition to the climate-implicit model described in the main text.  
697 Identifying the potentially complex relationships between vital rates and environmen-  
698 tal drivers remains a key challenge for accurate forecasts of the ecological impacts of  
699 environmental stochasticity [64]. We first downloaded temperature and precipitation  
700 data from a weather station in Bloomington, IN, approx. 27 km from our study site,  
701 using the rnoaa package [65]. Compared to other weather stations in the area, the  
702 measurements from Bloomington contain the most complete climate record across the  
703 study period and are correlated with more local measurements from Nashville, IN for  
704 years in which local data are available (total daily precipitation:  $R^2 = .76$ ; mean daily  
705 temperature:  $R^2 = .94$ ). The mean annual temperature across the study period was  
706  $11.9 C^\circ$  (SD:  $1.05 C^\circ$ ) and the average annual precipitation was 1237.9 mm/year (SD:  
707 204.89 mm/year) (Fig. A24). Given the known role of endophytes in promoting host  
708 drought tolerance, we calculated the Standardised Precipitation-Evapotranspiration  
709 Index (SPEI) for 3 and 12 months preceding each annual censuses, reflecting drought  
710 during the growing season and across the year [50]. To calculate SPEI, we used the  
711 Thornthwaite equation to model potential evapotranspiration as implemented in the  
712 SPEI R package [66]

713 We repeated the process of fitting statistical models for each vital rate as described  
714 in **Materials and Methods** with the inclusion of a parameter describing the influ-  
715 ence of SPEI. We fit separate vital rate models incorporating either the growing season  
716 or annual drought index for each vital rate, except for the model describing the mean  
717 number of seeds per inflorescence. This model was fit without climate effects because  
718 the data came from only a few years. Initial analyses indicated similar fits for models  
719 including only a linear term and those with both linear and quadratic terms describ-  
720 ing the relationship between the climate driver and the vital rate response, and so  
721 we proceeded with models including only the linear term. We expected that includ-  
722 ing climate predictors into the models would explain some inter-annual variance in  
723 vital rates, shrinking the variance associated with the fitted year random effects. We  
724 assessed model fit with graphic posterior predictive checks and convergence diagnostics  
725 as described for the climate-implicit analysis. Finally, we next built matrix projec-  
726 tion models incorporating the climate-dependent vital rate functions to assess the  
727 response of symbiotic (S+) vs symbiont-free (S-) populations to drought. The model  
728 is as described in **Materials and Methods** with the inclusion of parameters describ-  
729 ing the slope of the relationship with SPEI. We compared the sensitivity of  $\lambda$  to either  
730 annual or seasonal SPEI of S+ populations ( $\frac{\Delta\lambda^+}{\Delta SPEI}$ ) with those of S- populations  
731 ( $\frac{\Delta\lambda^-}{\Delta SPEI}$ ) (Fig. S25; Table S).

732 Most species were slightly more responsive to growing season rather than annual  
733 drought conditions, and for most species symbiotic populations were less sensitive to  
734 SPEI than symbiont-free populations (Fig. S25; Table S3). However, these drought  
735 indices did not explain the full extent of inter-annual variability in demographic  
736

vital rates. For example, flowering in *A. perennans* had one of the strongest climate signals (82% probability of a positive relationship with SPEI), yet the estimated inter-annual variance  $\sigma_{\tau_P}^2$  for symbiont-free plants shrank from 6.7 to 6.1 after including 3-month SPEI as a covariate, suggesting that other factors contribute to inter-annual variability. 737  
738  
739  
740  
741  
742  
743  
744  
745  
746  
747  
748  
749  
750  
751  
752  
753  
754  
755  
756  
757  
758  
759  
760  
761  
762  
763  
764  
765  
766  
767  
768  
769  
770  
771  
772  
773  
774  
775  
776  
777  
778  
779  
780  
781  
782

## 783 Supplemental Figures A1-A28

784

785

786

787

788

789

790

791

792

793

794

795

796

797

798

799

800

801

802

803

804

805

806

807

808

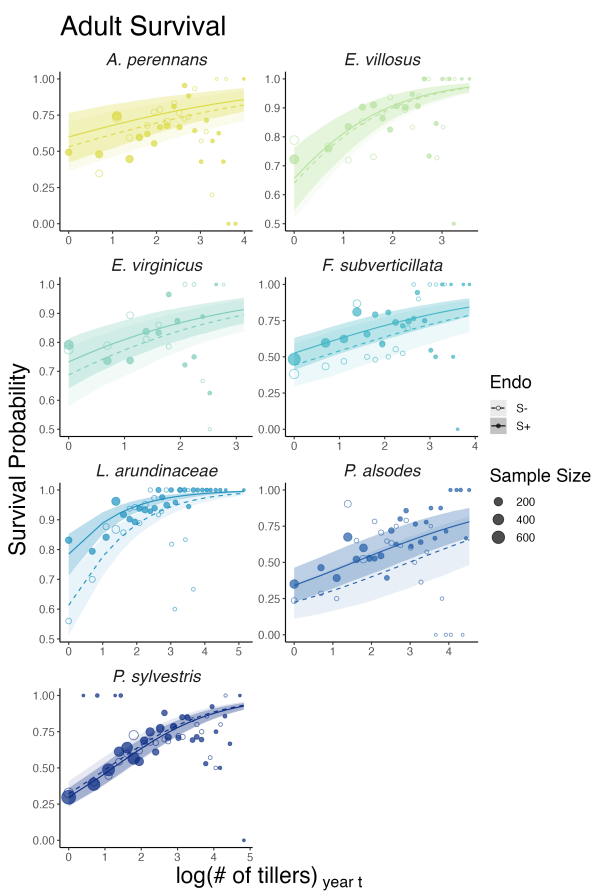
809

810

811

812

813



814 **Fig. 1** Effect of endophyte symbiosis on mean adult survival. Fitted curves represent the size-specific  
 815 mean survival probability along with data binned by size shown as open circles with a dashed line  
 816 for symbiont-free (S-) plants, while the solid line and filled circles represent symbiotic (S+) plants.  
 817 80% credible intervals are shown with dark shading for S+, or light shading for S-.

818

819

820

821

822

823

824

825

826

827

828

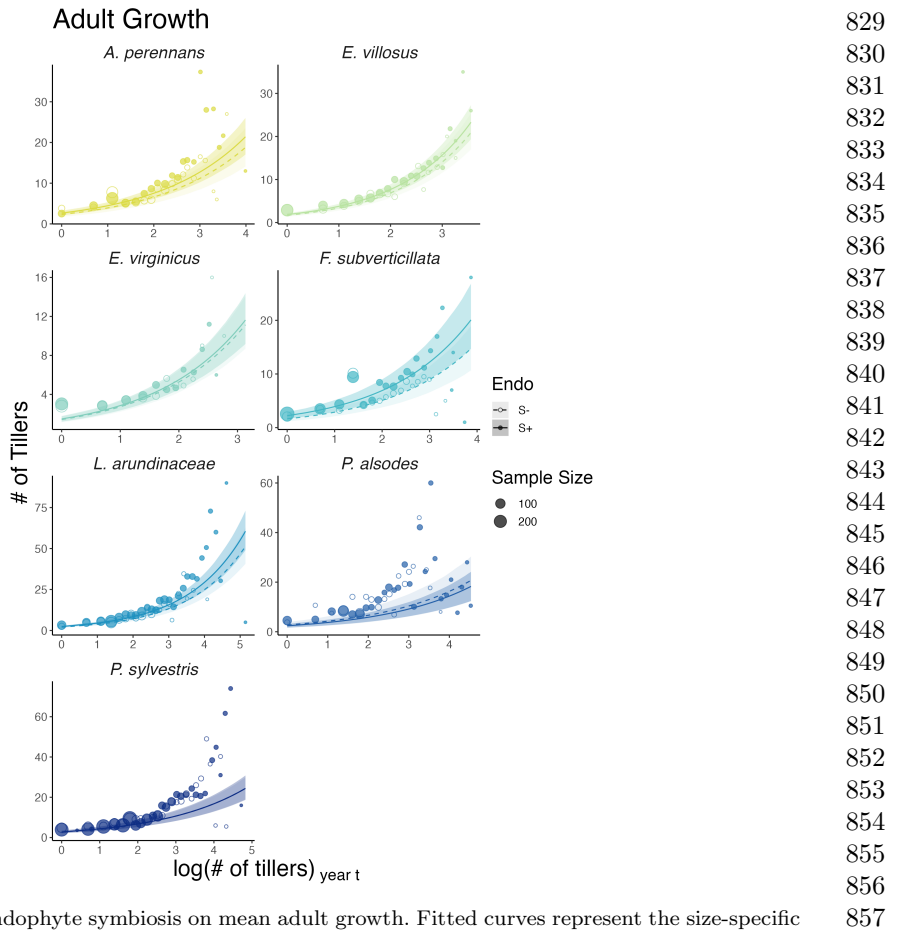
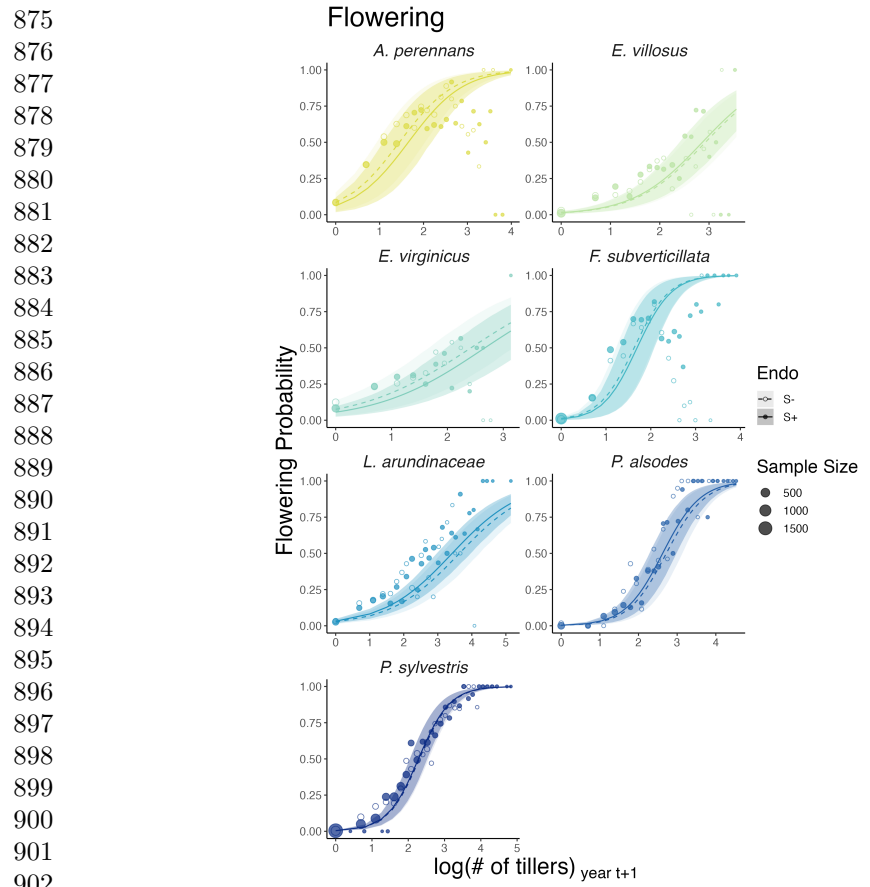


**Fig. 2** Effect of endophyte symbiosis on mean adult growth. Fitted curves represent the size-specific mean expected plant size along with data binned by size shown as open circles with a dashed line for symbiont-free (S-) plants, while the solid line and filled circles represent symbiotic (S+) plants. 80% credible intervals are shown with dark shading for S+, or light shading for S-. 829  
830  
831  
832  
833  
834  
835  
836  
837  
838  
839  
840  
841  
842  
843  
844  
845  
846  
847  
848  
849  
850  
851  
852  
853  
854  
855  
856  
857  
858  
859  
860  
861  
862  
863  
864  
865  
866  
867  
868  
869  
870  
871  
872  
873  
874



903 **Fig. 3** Effect of endophyte symbiosis on mean flowering. Fitted curves represent the size-specific  
 904 mean flowering probability along with data binned by size shown as open circles with a dashed line  
 905 for symbiont-free (S-) plants, while the solid line and filled circles represent symbiotic (S+) plants.  
 906 80% credible intervals are shown with dark shading for S+, or light shading for S-.

907

908

909

910

911

912

913

914

915

916

917

918

919

920

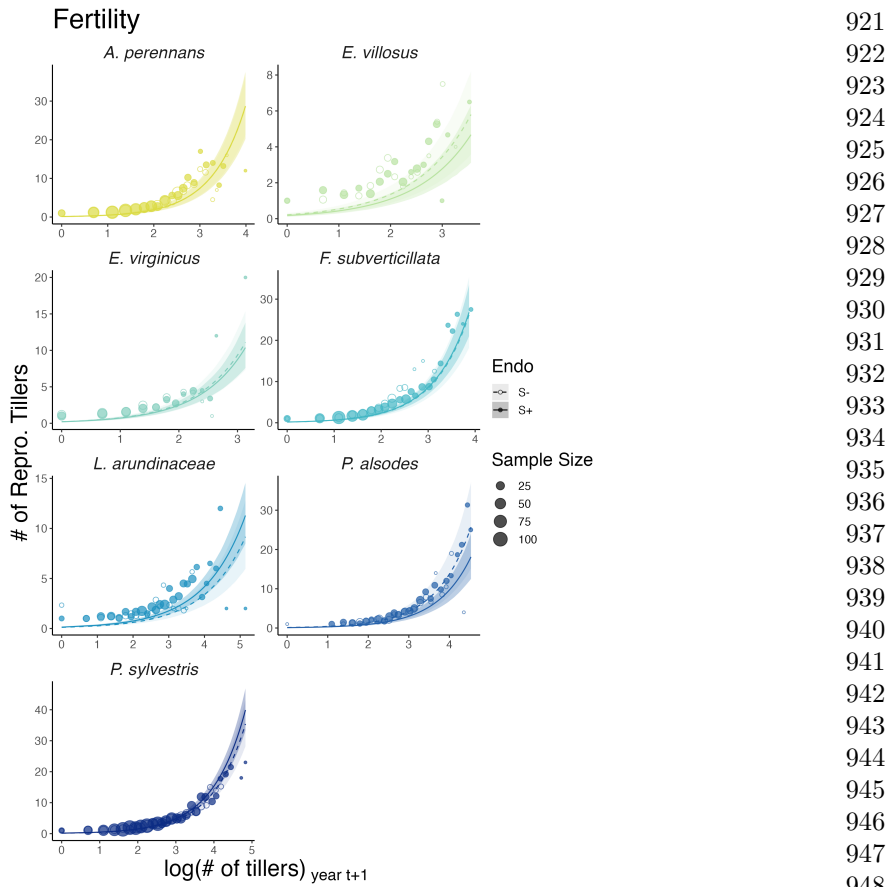
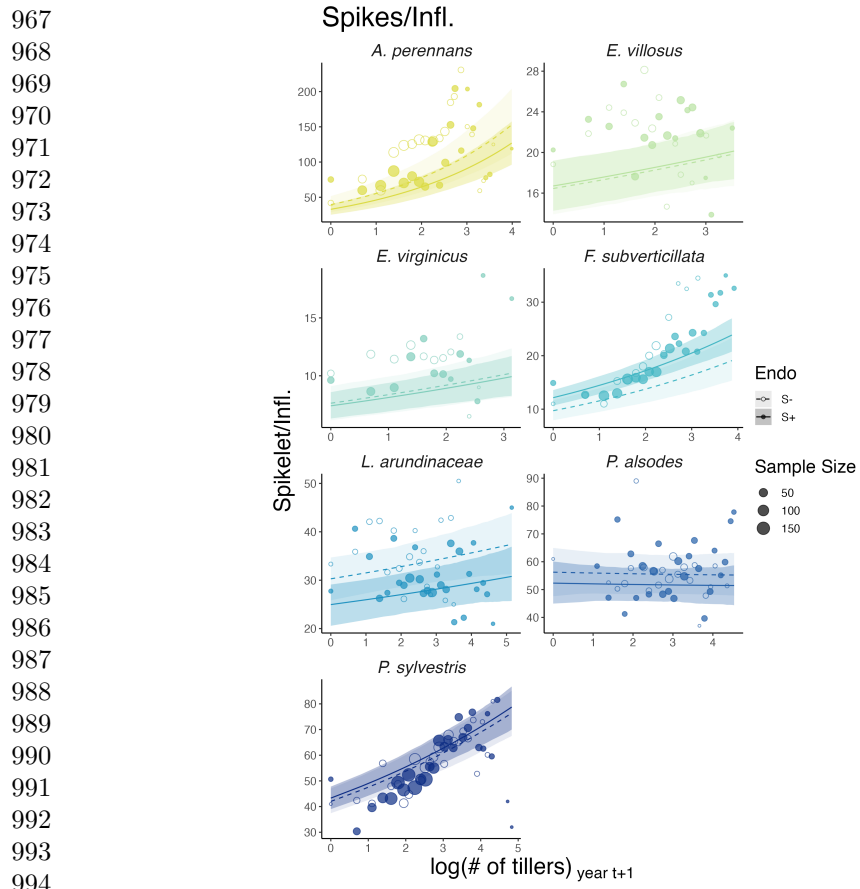


**Fig. 4** Effect of endophyte symbiosis on mean fertility. Fitted curves represent the size-specific mean expected number of flowering tillers along with data binned by size shown as open circles with a dashed line for symbiont-free (S-) plants, while the solid line and filled circles represent symbiotic (S+) plants. 80% credible intervals are shown with dark shading for S+, or light shading for S-.



995 **Fig. 5** Effect of endophyte symbiosis on mean spikelet production. Fitted curves represent the size-  
 996 specific mean expected number of spikelets per inflorescence along with data binned by size shown  
 997 as open circles with a dashed line for symbiont-free (S-) plants, while the solid line and filled circles  
 998 represent symbiotic (S+) plants. 80% credible intervals are shown with dark shading for S+, or light  
 999 shading for S-.  
 1000  
 1001  
 1002  
 1003  
 1004  
 1005  
 1006  
 1007  
 1008  
 1009  
 1010  
 1011  
 1012

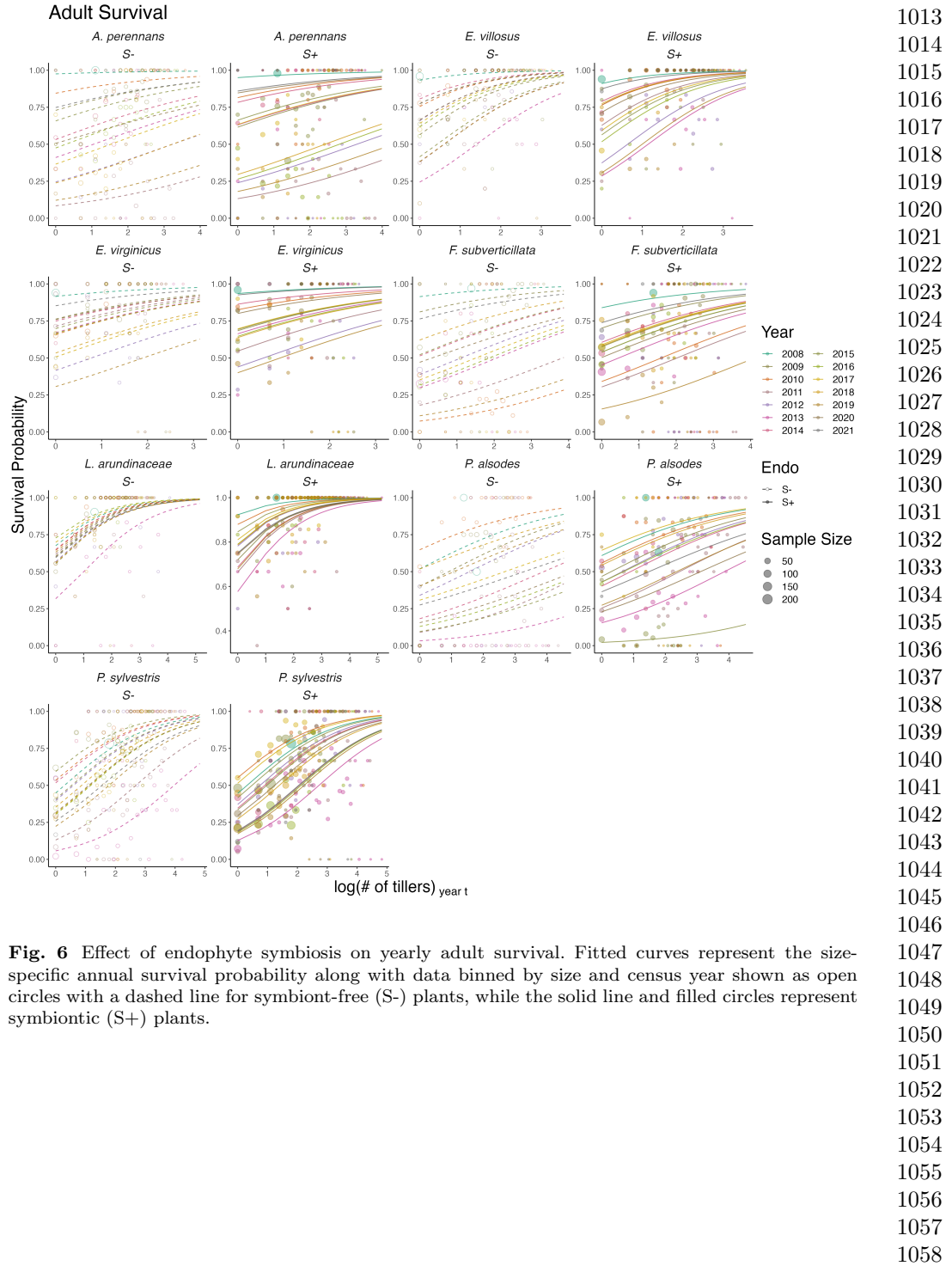
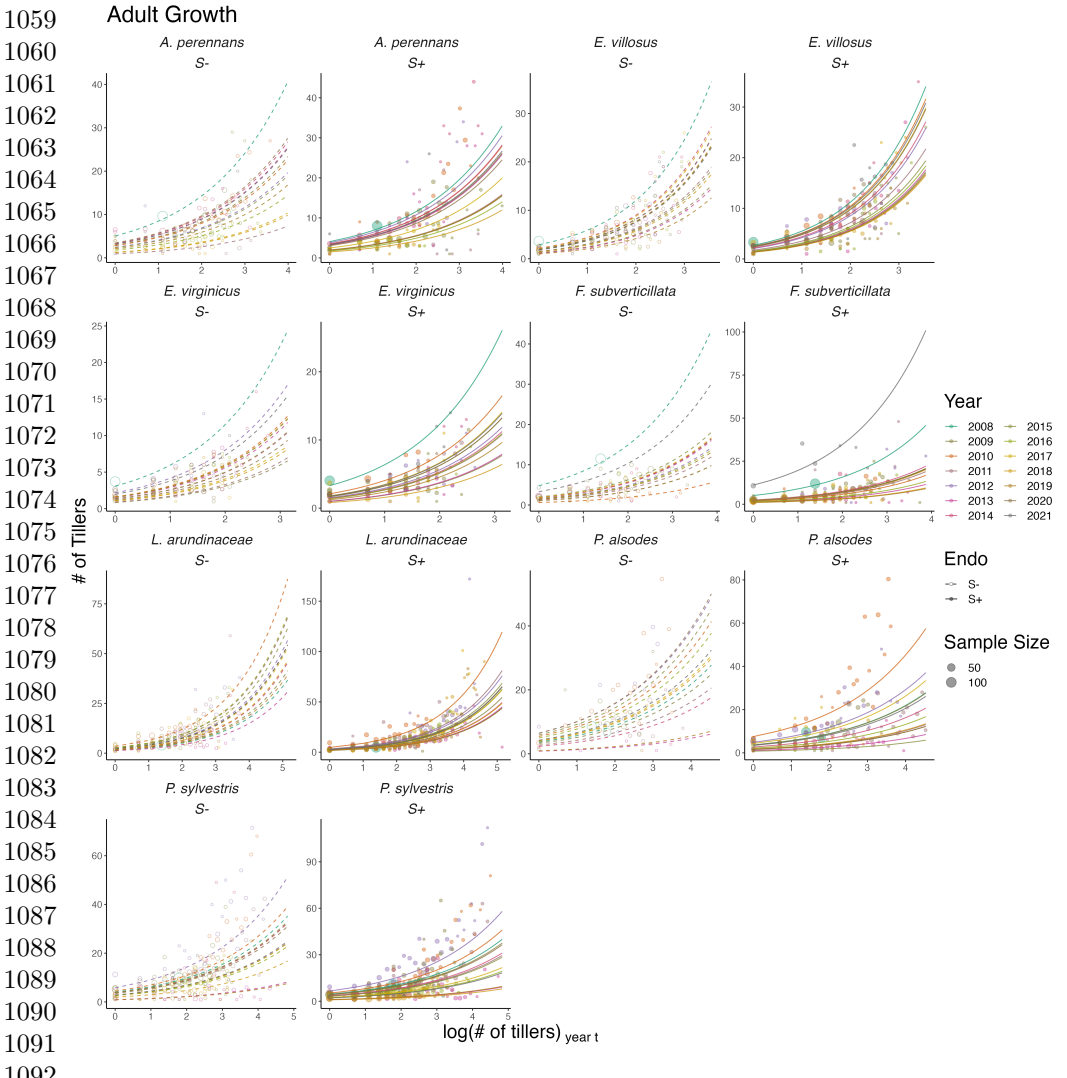
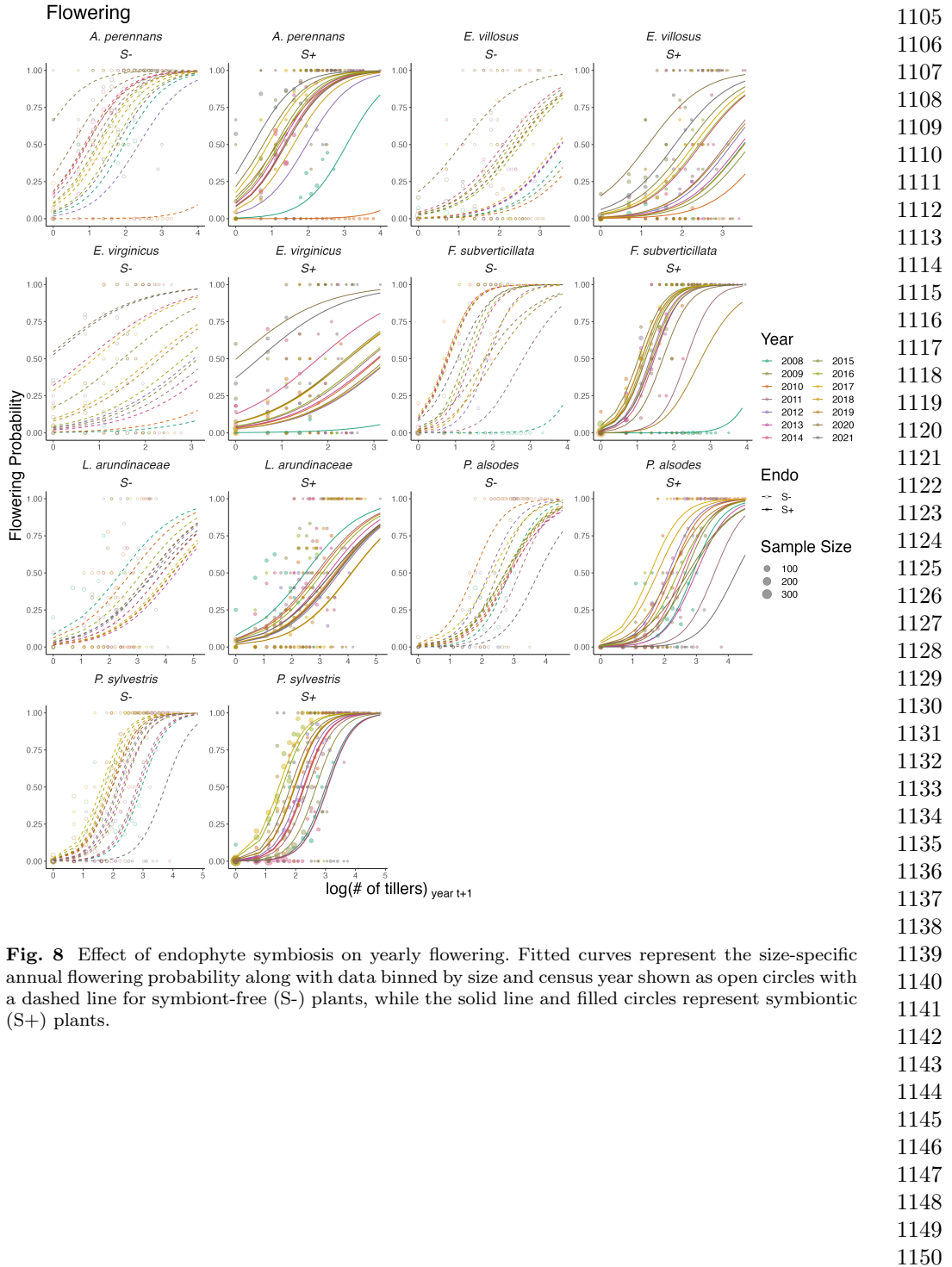


**Fig. 6** Effect of endophyte symbiosis on yearly adult survival. Fitted curves represent the size-specific annual survival probability along with data binned by size and census year shown as open circles with a dashed line for symbiont-free (S-) plants, while the solid line and filled circles represent symbiotic (S+) plants.

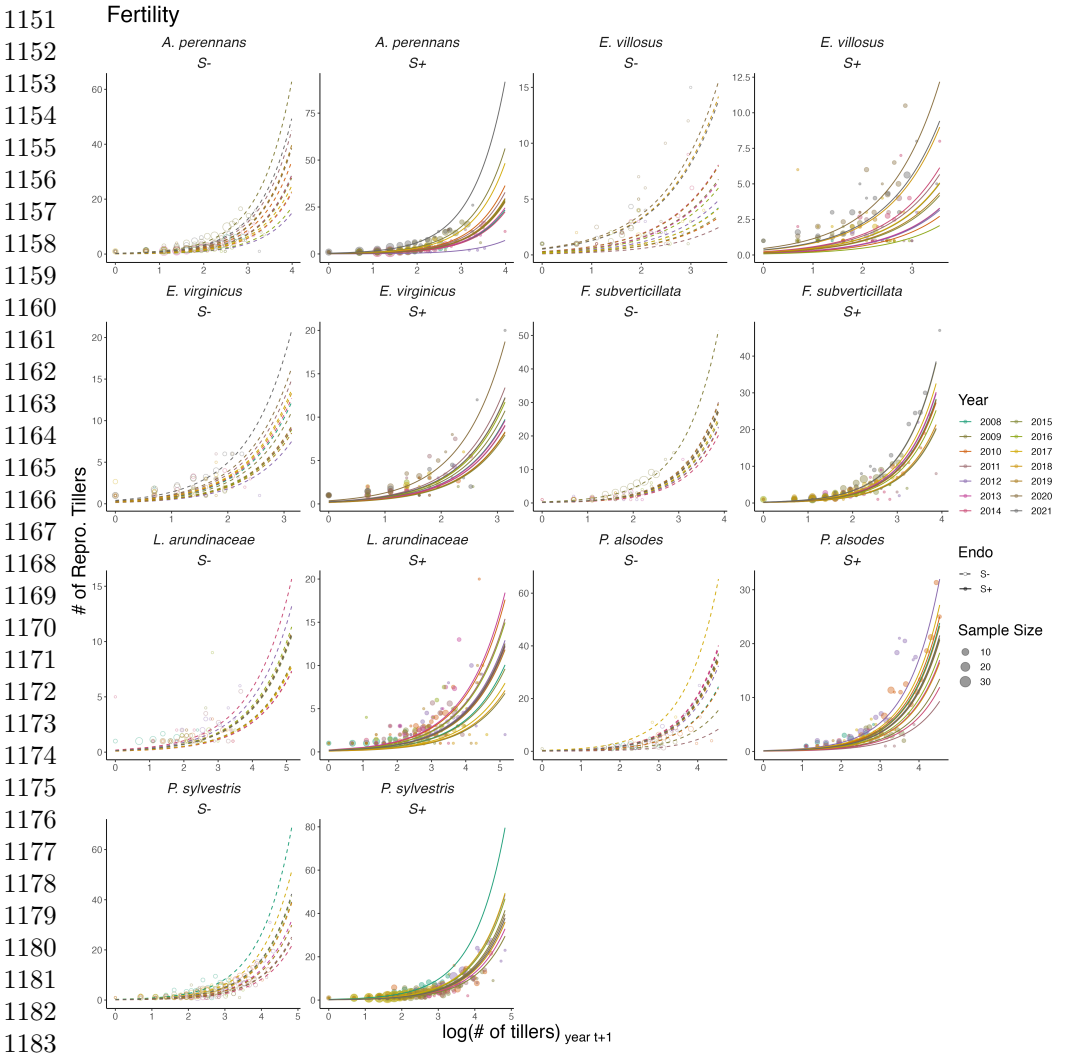


1093 **Fig. 7** Effect of endophyte symbiosis on yearly adult growth. Fitted curves represent the size-specific  
 1094 annual expected plant size along with data binned by size and census year shown as open circles with  
 1095 a dashed line for symbiont-free (S-) plants, while the solid line and filled circles represent symbiotic  
 1096 (S+) plants.

1097  
 1098  
 1099  
 1100  
 1101  
 1102  
 1103  
 1104



**Fig. 8** Effect of endophyte symbiosis on yearly flowering. Fitted curves represent the size-specific annual flowering probability along with data binned by size and census year shown as open circles with a dashed line for symbiont-free (S-) plants, while the solid line and filled circles represent symbiotic (S+) plants.



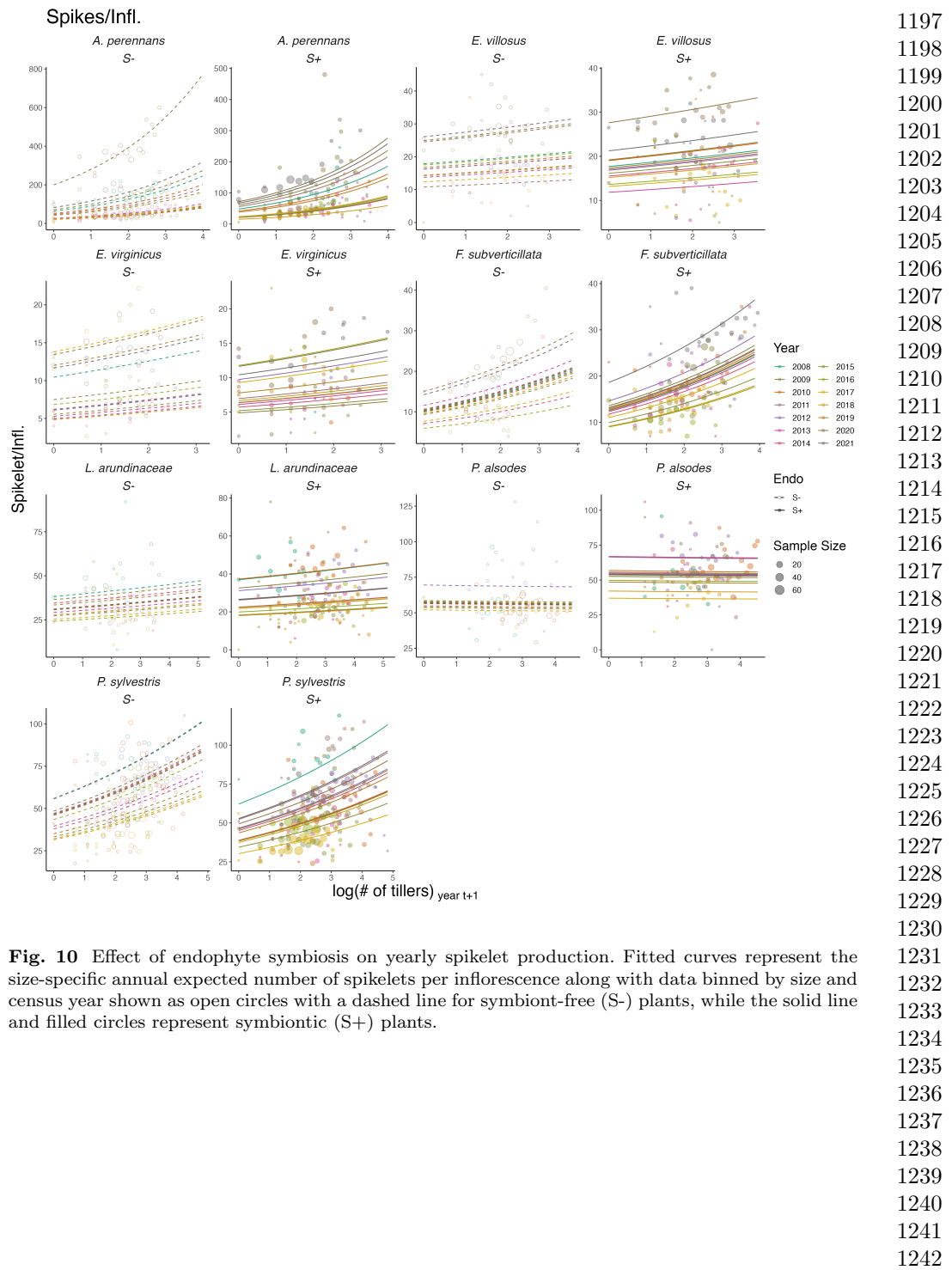
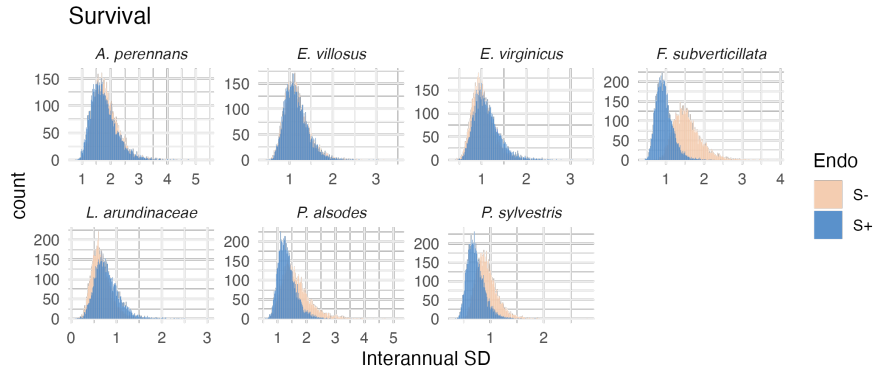


**Fig. 10** Effect of endophyte symbiosis on yearly spikelet production. Fitted curves represent the size-specific annual expected number of spikelets per inflorescence along with data binned by size and census year shown as open circles with a dashed line for symbiont-free (S-) plants, while the solid line and filled circles represent symbiotic (S+) plants.



1255 **Fig. 11** Posterior distributions of the standard deviations of inter-annual year effects for survival.  
 1256 Histograms include 7500 post-warmup MCMC samples for symbiotic (S+; blue) and symbiont-free  
 1257 (S-; tan) plants from fitted vital rate model.

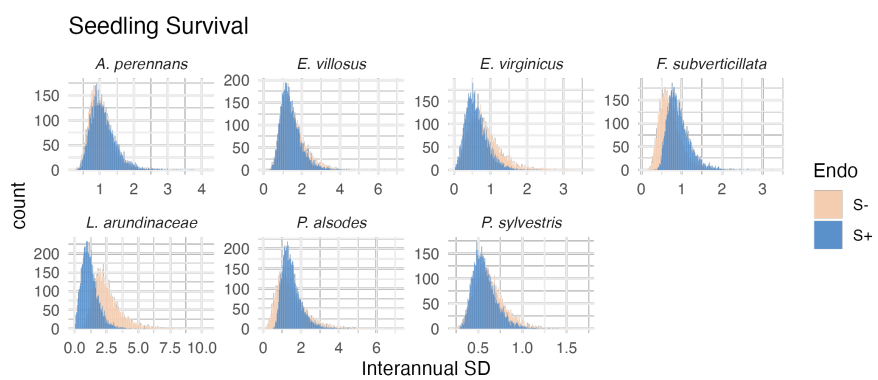


**Fig. 12** Posterior distributions of the standard deviations of inter-annual year effects for seedling survival. Histograms include 7500 post-warmup MCMC samples for symbiotic (S+; blue) and symbiont-free (S-; tan) plants from fitted vital rate model.

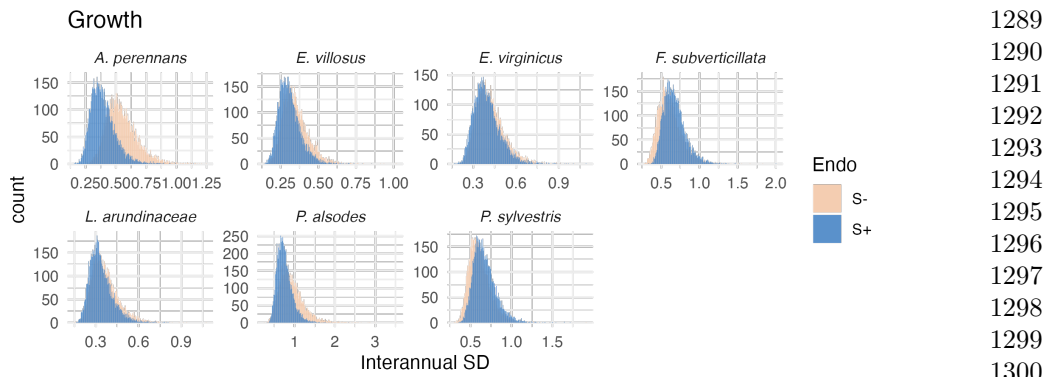


**Fig. 13** Posterior distributions of the standard deviations of inter-annual year effects for growth. Histograms include 7500 post-warmup MCMC samples for symbiotic (S+; blue) and symbiont-free (S-; tan) plants from fitted vital rate model.

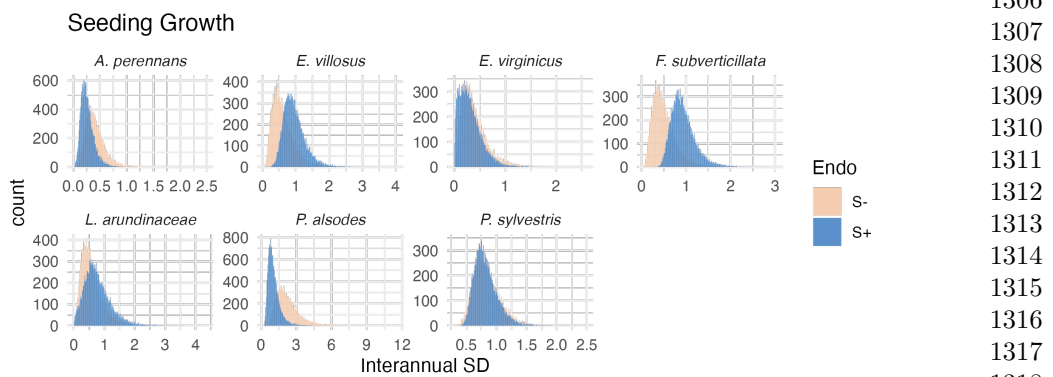


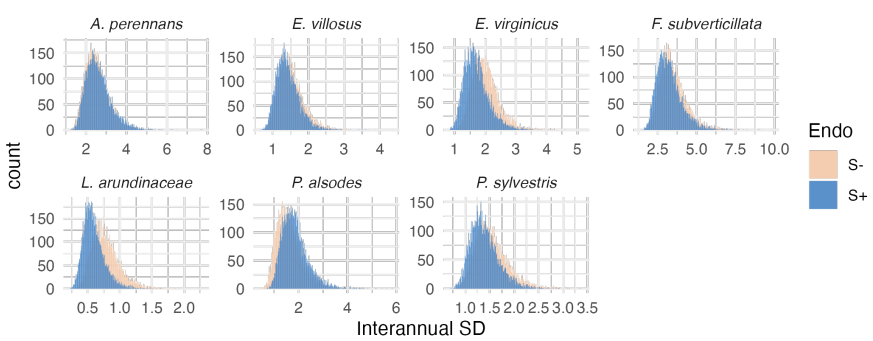
**Fig. 14** Posterior distributions of the standard deviations of inter-annual year effects for seedling growth. Histograms include 7500 post-warmup MCMC samples for symbiotic (S+; blue) and symbiont-free (S-; tan) plants from fitted vital rate model.

1289  
1290  
1291  
1292  
1293  
1294  
1295  
1296  
1297  
1298  
1299  
1300  
1301  
1302  
1303  
1304  
1305  
1306  
1307  
1308  
1309  
1310  
1311  
1312  
1313  
1314  
1315  
1316  
1317  
1318  
1319  
1320  
1321  
1322  
1323  
1324  
1325  
1326  
1327  
1328  
1329  
1330  
1331  
1332  
1333  
1334

1335

**Flowering**

1336



1347

**Fig. 15** Posterior distributions of the standard deviations of inter-annual year effects for flowering probability. Histograms include 7500 post-warmup MCMC samples for symbiotic (S+; blue) and symbiont-free (S-; tan) plants from fitted vital rate model.

1348

1349

1350

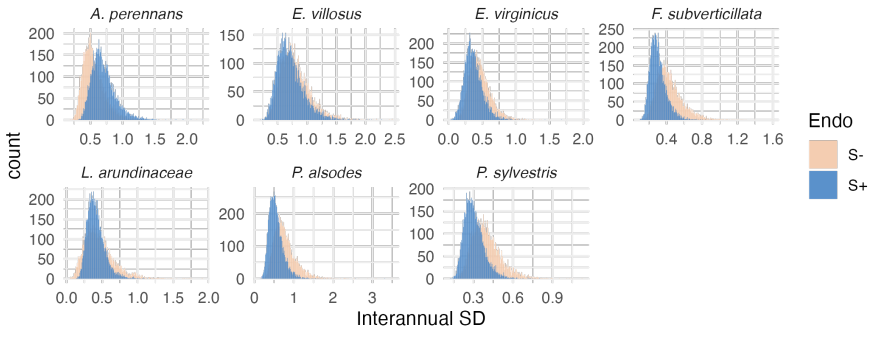
1351

1352

1353

**# of Flw Tillers**

1354



1364

1365

**Fig. 16** Posterior distributions of the standard deviations of inter-annual year effects for fertility (no. of flowering tillers). Histograms include 7500 post-warmup MCMC samples for symbiotic (S+; blue) and symbiont-free (S-; tan) plants from fitted vital rate model.

1366

1367

1368

1369

1370

1371

1372

1373

1374

1375

1376

1377

1378

1379

1380

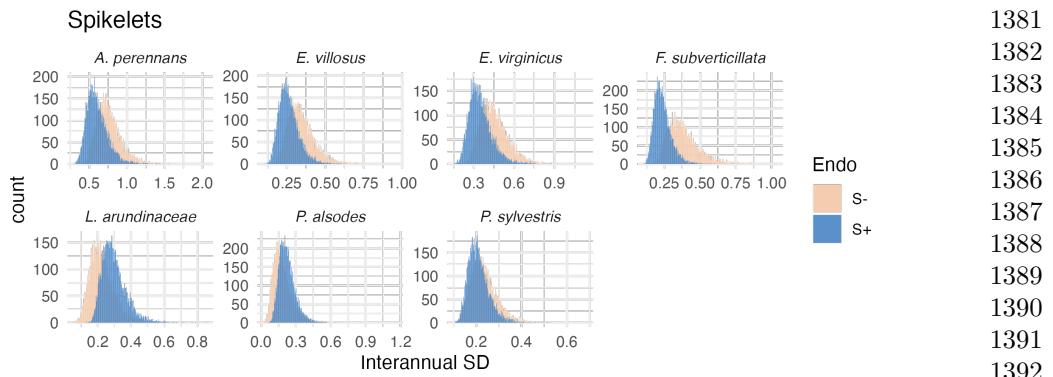


**Fig. 17** Posterior distributions of the standard deviations of inter-annual year effects for spikelets per inflorescence. Histograms include 7500 post-warmup MCMC samples for symbiotic (S+; blue) and symbiont-free (S-; tan) plants from fitted vital rate model.

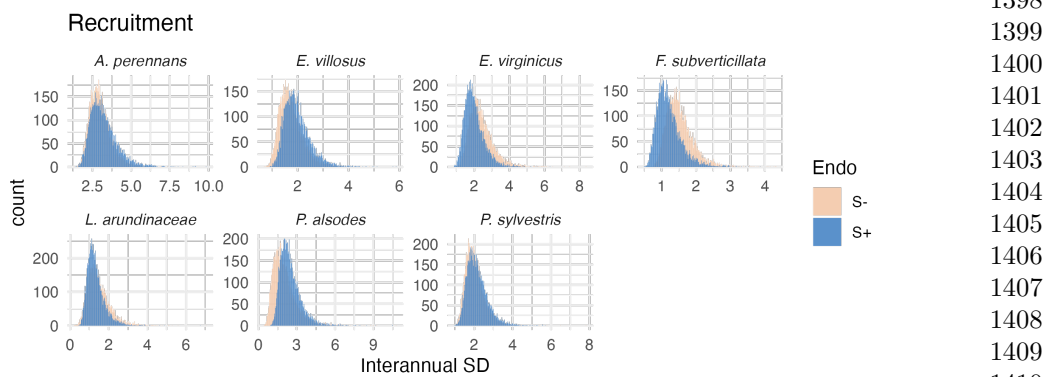
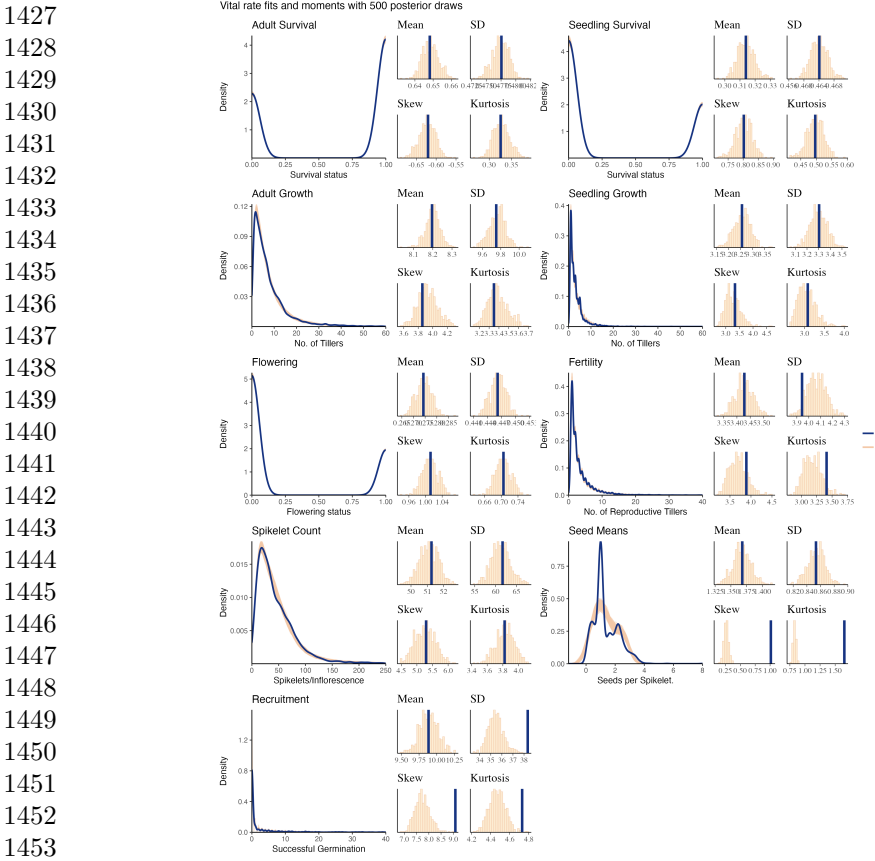


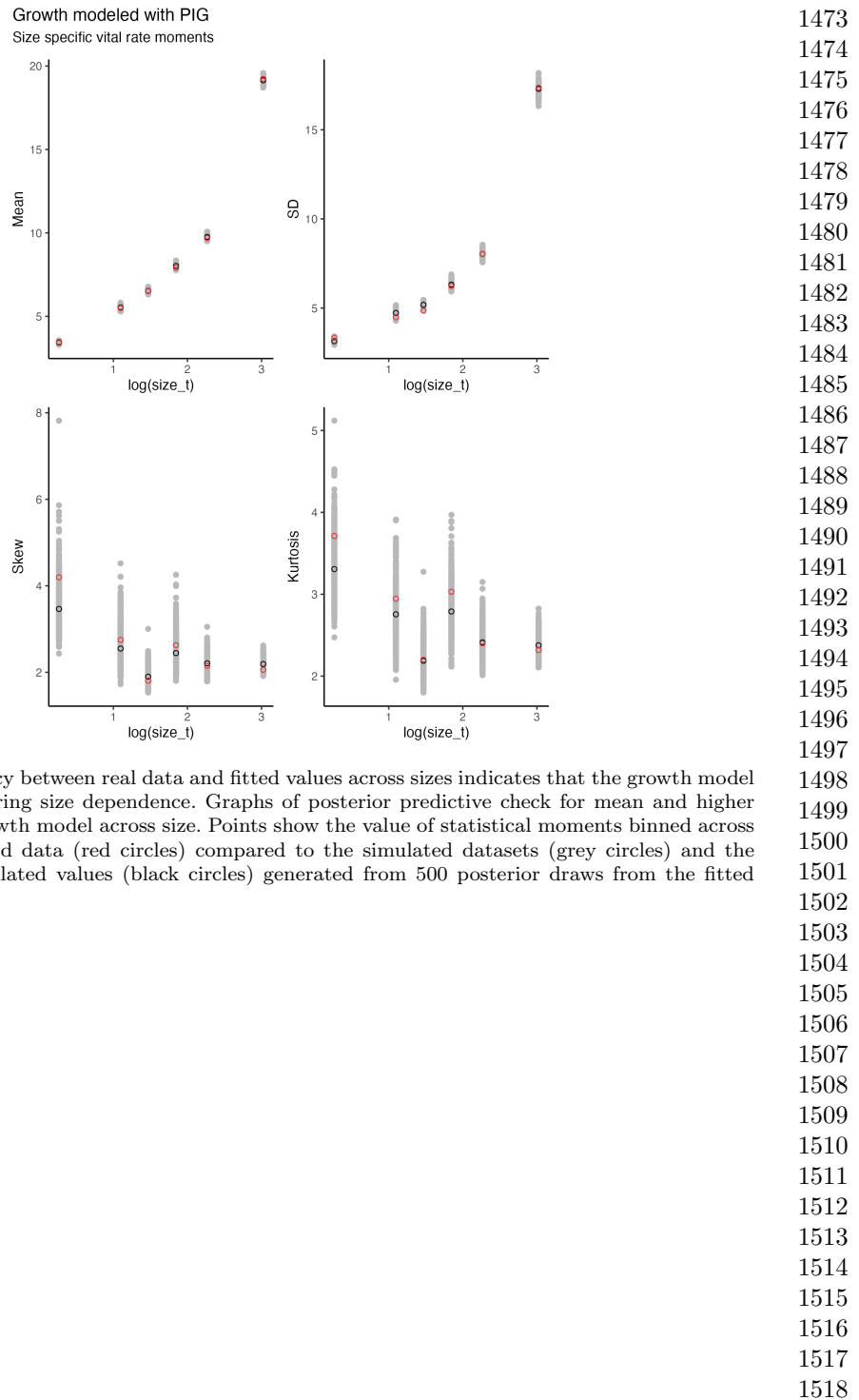
**Fig. 18** Posterior distributions of the standard deviations of inter-annual year effects for recruitment. Histograms include 7500 post-warmup MCMC samples for symbiotic (S+; blue) and symbiont-free (S-; tan) plants from fitted vital rate model.

|      |
|------|
| 1381 |
| 1382 |
| 1383 |
| 1384 |
| 1385 |
| 1386 |
| 1387 |
| 1388 |
| 1389 |
| 1390 |
| 1391 |
| 1392 |
| 1393 |
| 1394 |
| 1395 |
| 1396 |
| 1397 |
| 1398 |
| 1399 |
| 1400 |
| 1401 |
| 1402 |
| 1403 |
| 1404 |
| 1405 |
| 1406 |
| 1407 |
| 1408 |
| 1409 |
| 1410 |
| 1411 |
| 1412 |
| 1413 |
| 1414 |
| 1415 |
| 1416 |
| 1417 |
| 1418 |
| 1419 |
| 1420 |
| 1421 |
| 1422 |
| 1423 |
| 1424 |
| 1425 |
| 1426 |

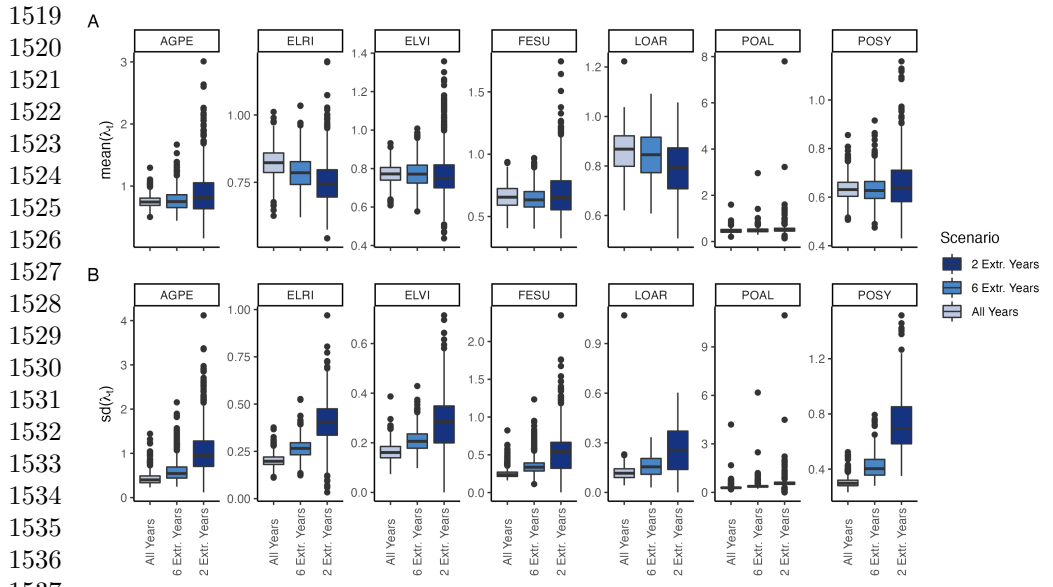


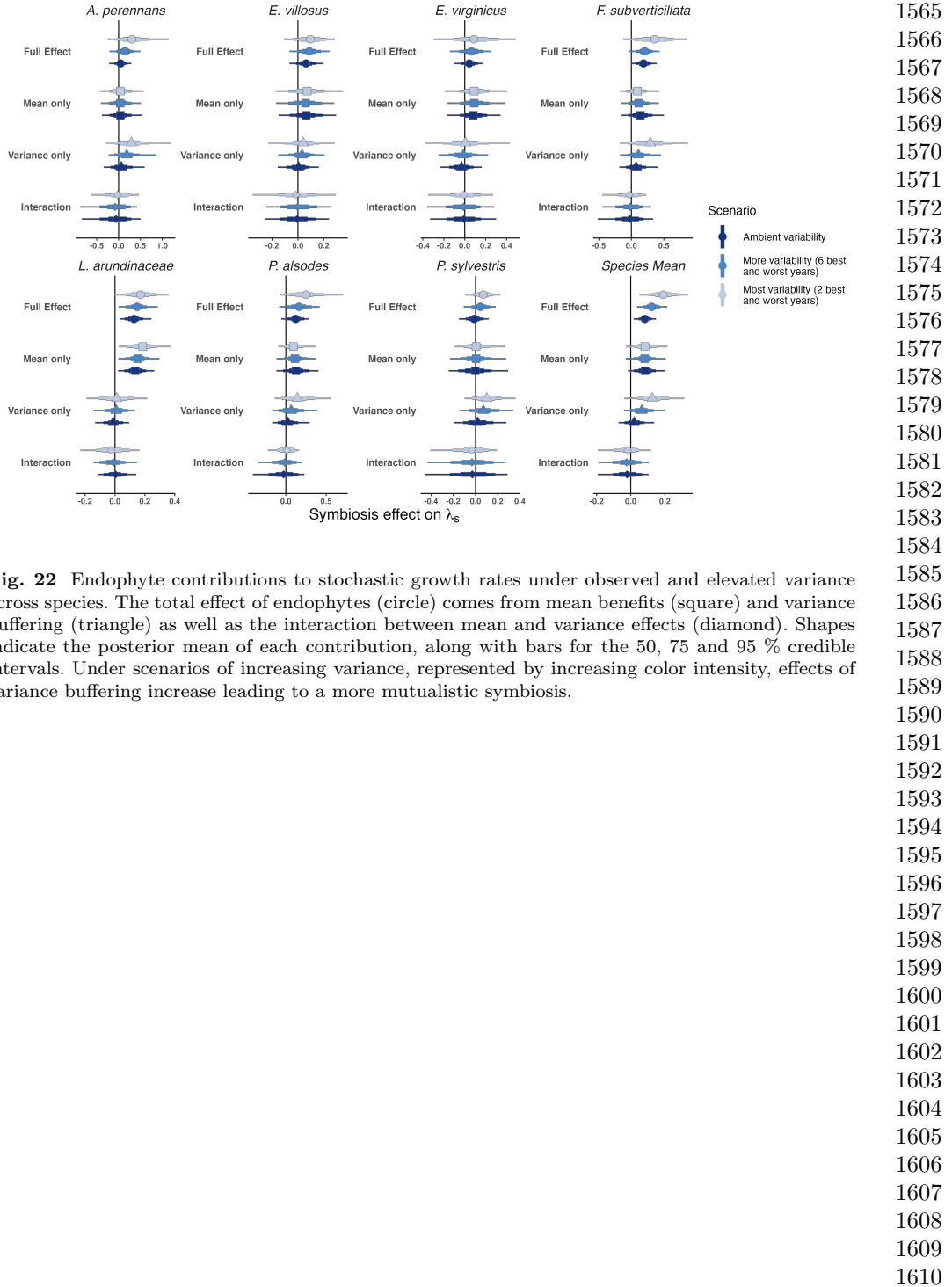
1454 **Fig. 19** Consistency between real data and simulated values indicates that fitted models describe  
1455 the data well. Graphs show posterior predictive check for statistical models of demographic vital  
1456 rates. Lines show density distributions of observed data (blue line) compared to data simulated from  
1457 fitted models (tan lines) generated from 500 draws from posterior distributions of model parameters.

1458  
1459  
1460  
1461  
1462  
1463  
1464  
1465  
1466  
1467  
1468  
1469  
1470  
1471  
1472

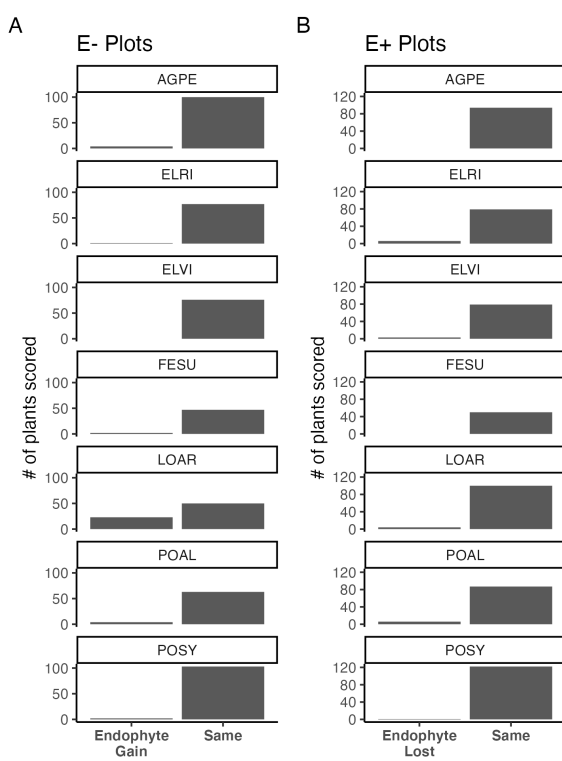


**Fig. 20** Consistency between real data and fitted values across sizes indicates that the growth model is accurately capturing size dependence. Graphs of posterior predictive check for mean and higher moments of the growth model across size. Points show the value of statistical moments binned across size for the observed data (red circles) compared to the simulated datasets (grey circles) and the median of the simulated values (black circles) generated from 500 posterior draws from the fitted model.





1611  
 1612  
 1613  
 1614  
 1615  
 1616  
 1617  
 1618  
 1619  
 1620  
 1621  
 1622  
 1623  
 1624  
 1625  
 1626  
 1627  
 1628  
 1629  
 1630  
 1631  
 1632  
 1633  
 1634  
 1635  
 1636  
 1637   **Fig. 23** Endophyte Status Checks  
 1638   Counts of plants scored with  
 1639   leaf peels or seed squashes to check the faithfulness of recruits to the assigned plot-level endophyte  
 1640   status. (A) Endophytic plants may be gained in initially S- plots, or (B) lost in initially S+ plots.  
 1641  
 1642  
 1643  
 1644  
 1645  
 1646  
 1647  
 1648  
 1649  
 1650  
 1651  
 1652  
 1653  
 1654  
 1655  
 1656



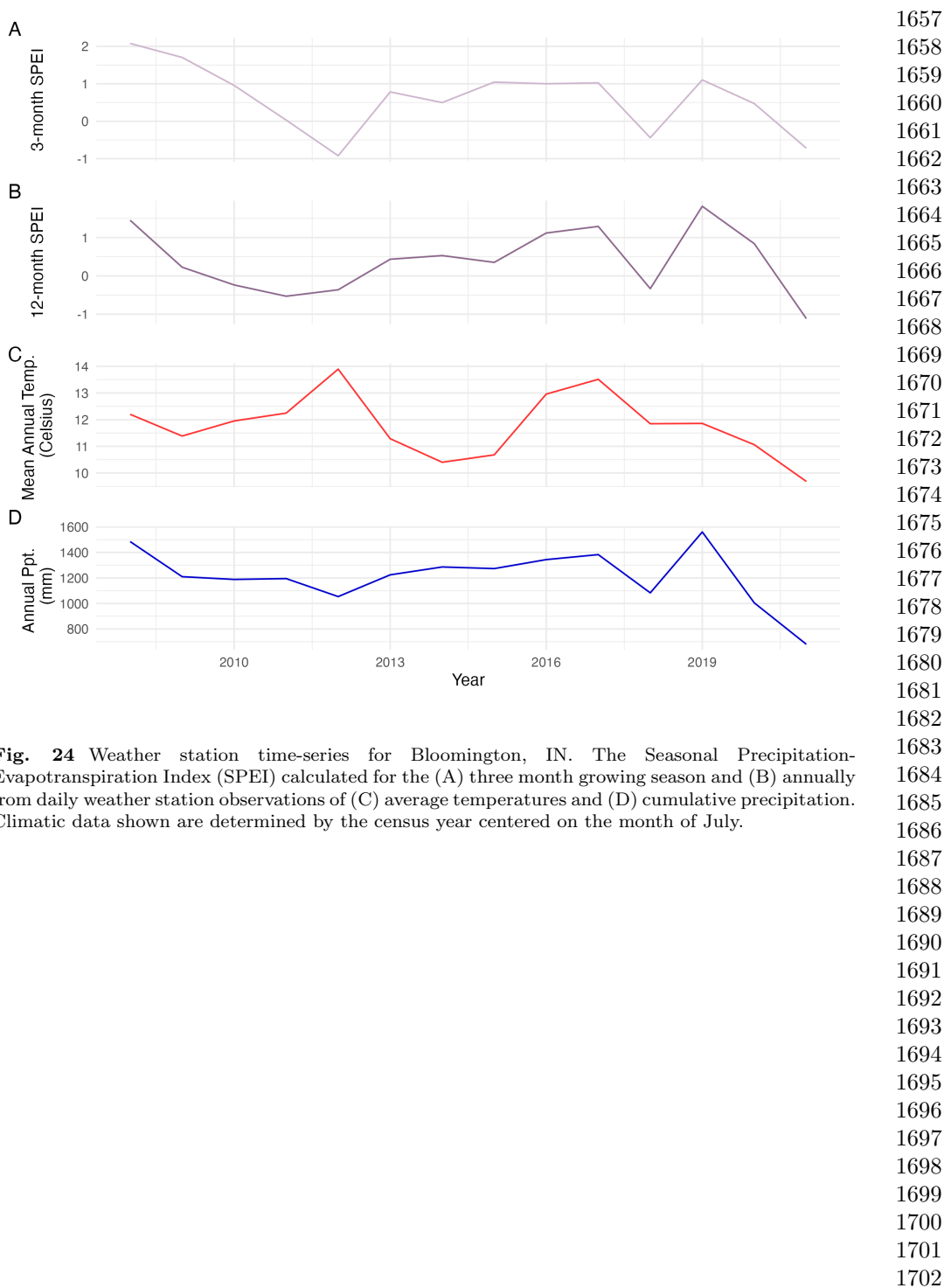
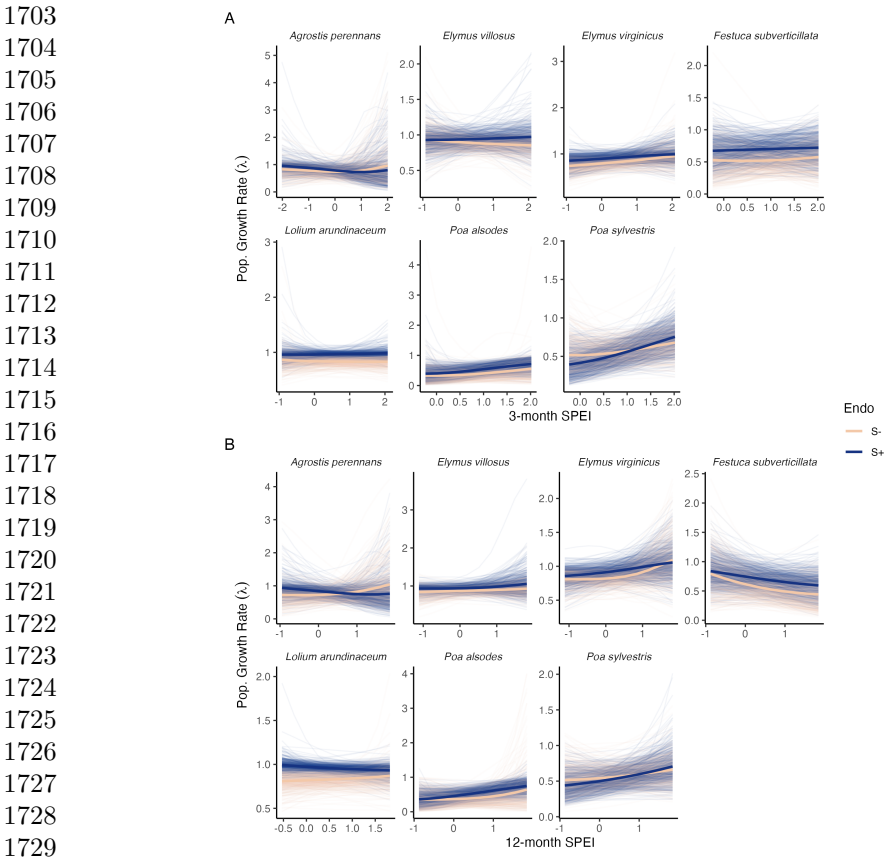


**Fig. 24** Weather station time-series for Bloomington, IN. The Seasonal Precipitation-Evapotranspiration Index (SPEI) calculated for the (A) three month growing season and (B) annually from daily weather station observations of (C) average temperatures and (D) cumulative precipitation. Climatic data shown are determined by the census year centered on the month of July.



1730 **Fig. 25** Predicted population growth rates across drought indices. Symbiotic (S+; blue) and  
1731 symbiont-free (S-; tan) populations respond differently to climate as measured by the (A) 3-month  
1732 SPEI and (B) 12-month SPEI. Thick lines represent the predicted mean growth rate and thin lines  
1733 show 500 posterior draws.

1734  
1735  
1736  
1737  
1738  
1739  
1740  
1741  
1742  
1743  
1744  
1745  
1746  
1747  
1748

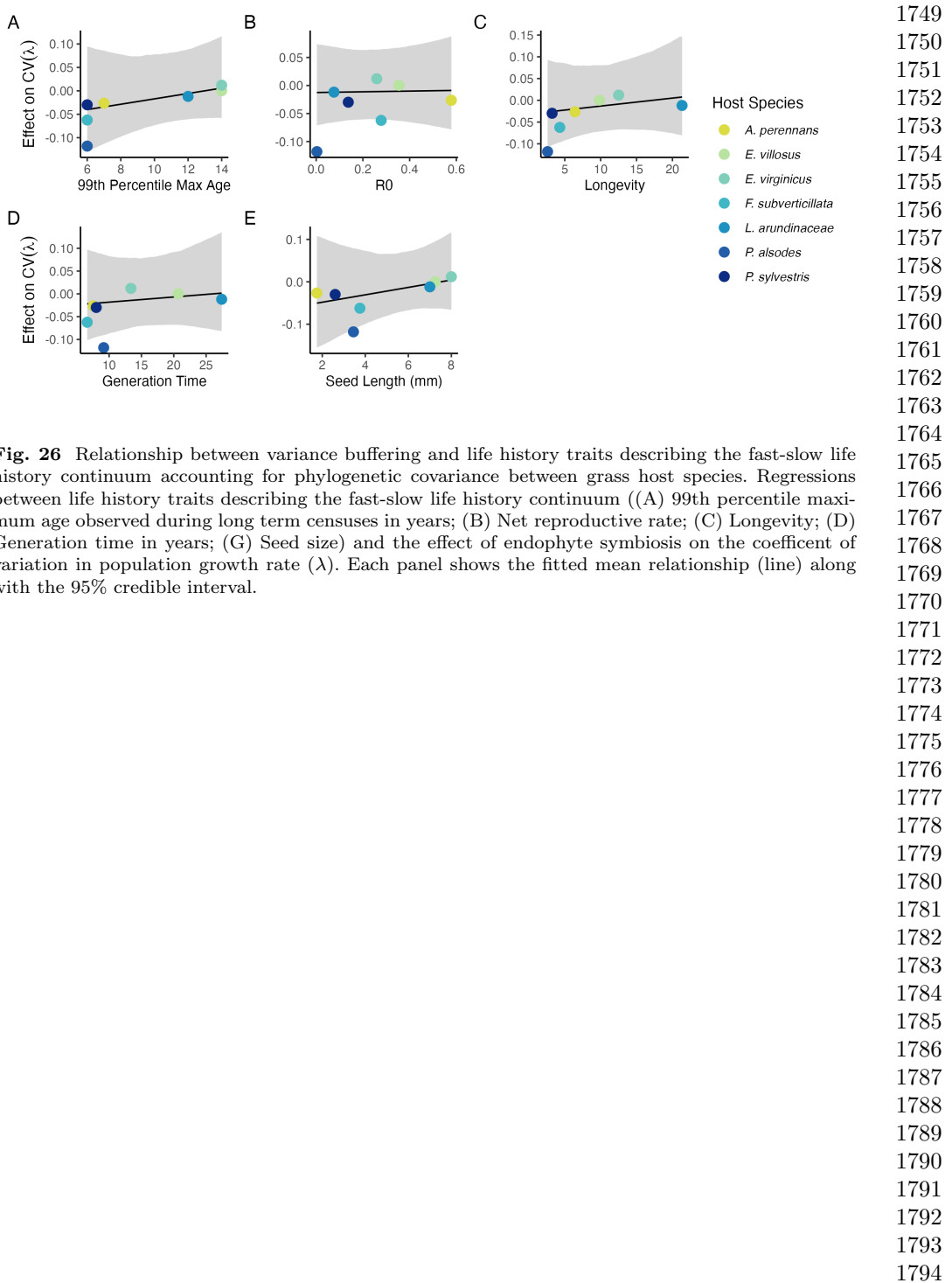


**Fig. 26** Relationship between variance buffering and life history traits describing the fast-slow life history continuum accounting for phylogenetic covariance between grass host species. Regressions between life history traits describing the fast-slow life history continuum ((A) 99th percentile maximum age observed during long term censuses in years; (B) Net reproductive rate; (C) Longevity; (D) Generation time in years; (E) Seed size) and the effect of endophyte symbiosis on the coefficient of variation in population growth rate ( $\lambda$ ). Each panel shows the fitted mean relationship (line) along with the 95% credible interval.

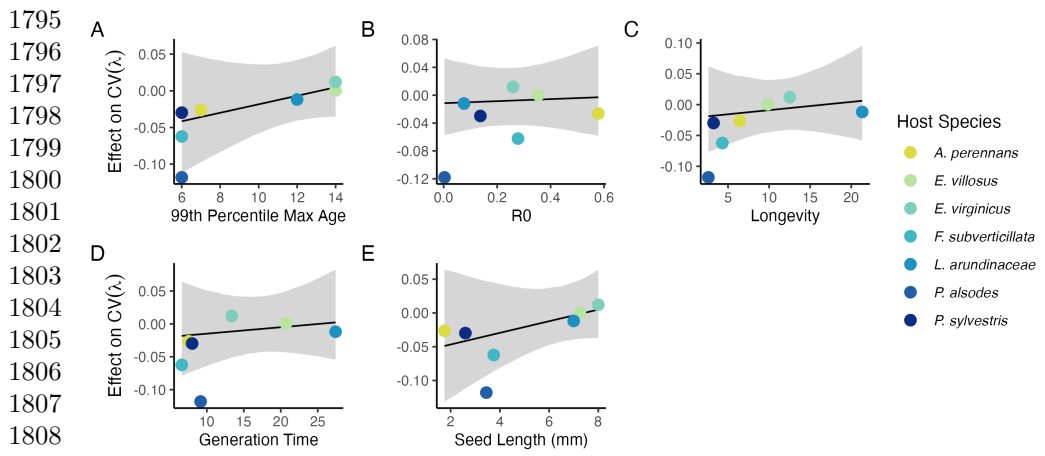


**Fig. 27** Relationship between variance buffering and life history traits describing the fast-slow life history continuum accounting for phylogenetic covariance between *Epichloë* symbionts. Regressions between life history traits describing the fast-slow life history continuum ((A) 99th percentile maximum age observed during long term censuses in years; (B) Net reproductive rate; (C) Longevity; (D) Generation time in years; (E) Seed size) and the effect of endophyte symbiosis on the coefficient of variation in population growth rate ( $\lambda$ ). Results are similar to regressions accounting for host plant phylogeny (Fig. A25), however symbionts are all within a single genus. Each panel shows the fitted mean relationship (line) along with the 95% credible interval.

1811  
 1812  
 1813  
 1814  
 1815  
 1816  
 1817  
 1818  
 1819  
 1820  
 1821  
 1822  
 1823  
 1824  
 1825  
 1826  
 1827  
 1828  
 1829  
 1830  
 1831  
 1832  
 1833  
 1834  
 1835  
 1836  
 1837  
 1838  
 1839  
 1840

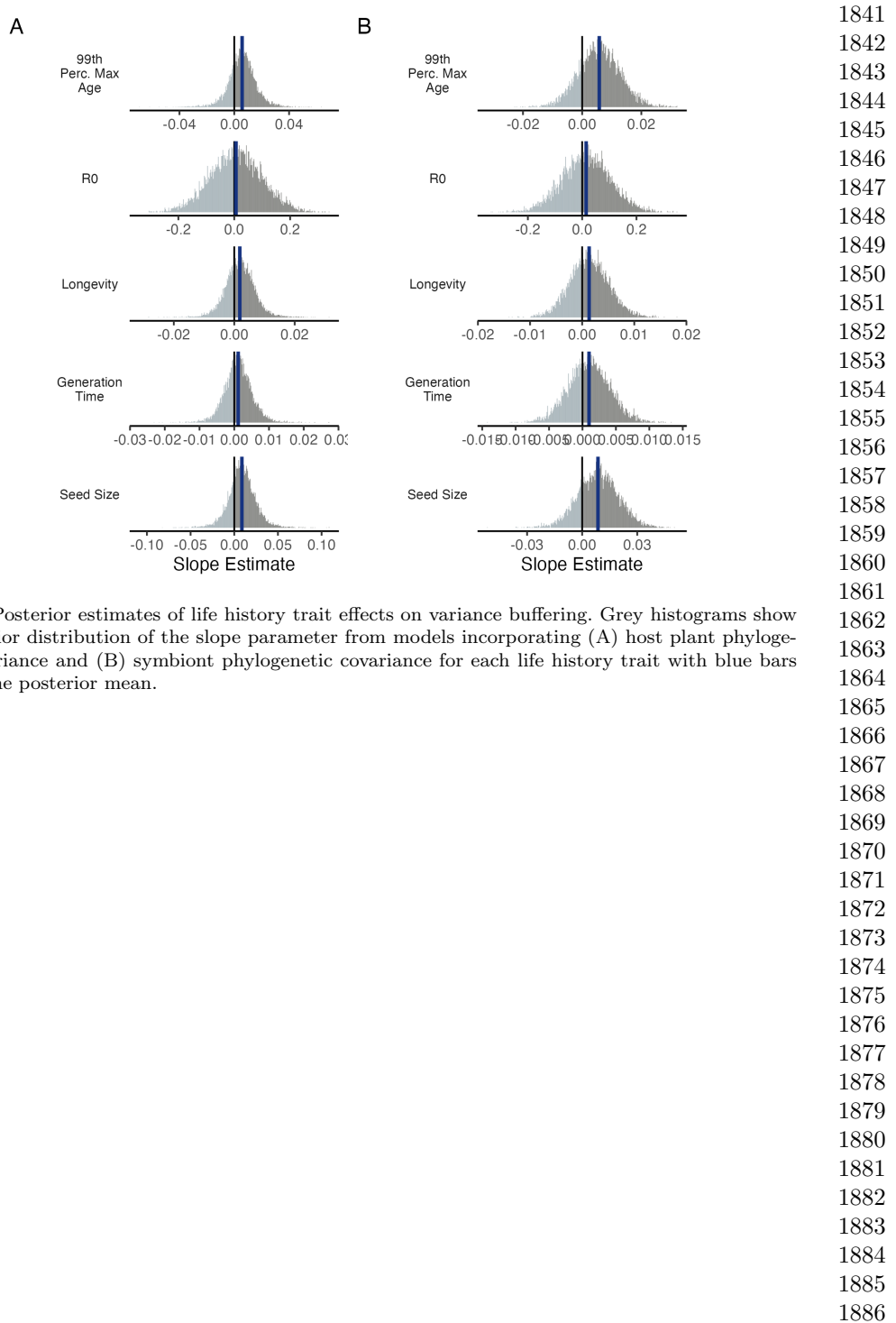


**Fig. 28** Posterior estimates of life history trait effects on variance buffering. Grey histograms show the posterior distribution of the slope parameter from models incorporating (A) host plant phylogenetic covariance and (B) symbiont phylogenetic covariance for each life history trait with blue bars showing the posterior mean.

**1887 Supplemental Tables A1-A3**

1888  
1889  
1890  
1891  
1892  
1893  
1894  
1895  
1896  
1897  
1898  
1899  
1900  
1901  
1902  
1903  
1904  
1905  
1906  
1907  
1908  
1909  
1910  
1911  
1912  
1913  
1914  
1915  
1916  
1917  
1918  
1919  
1920  
1921  
1922  
1923  
1924  
1925  
1926  
1927  
1928  
1929  
1930  
1931  
1932

1933  
1934  
1935  
1936  
1937  
1938  
1939  
1940  
1941  
1942  
1943  
1944  
1945  
1946  
1947  
1948  
1949  
1950  
1951  
1952  
1953  
1954  
1955  
1956  
1957  
1958  
1959  
1960  
1961  
1962  
1963  
1964  
1965  
1966  
1967  
1968  
1969  
1970  
1971  
1972  
1973  
1974  
1975  
1976  
1977  
1978

**Table 1** Summary of host-endophyte propagation and transplant methods

| Host Species                   | Symbiont Species                  | Heat treatment duration (Temp.) | Transplant date                            |
|--------------------------------|-----------------------------------|---------------------------------|--|
| <i>Agrostis perennans</i>      | <i>E. amarillans</i>              | 12 min. hot water bath (60 °C)  | April 2008 (10 plots)                      |
| <i>Elymus villosus</i>         | <i>E. elymi</i>                   | 6 days drying oven (60 °C)      | April 2008 (10 plots)                      |
| <i>Elymus virginicus</i>       | <i>E. elymi</i> or <i>EviTG-1</i> | 6 days drying oven (60 °C)      | April 2008 (10 plots)                      |
| <i>Festuca subverticillata</i> | <i>E. starrii</i>                 | 6 days drying oven (60 °C)      | April 2008 (10 plots)                      |
| <i>Lolium arundinaceum</i>     | <i>E. coenophiala</i>             | 6 days drying oven (60 °C)      | Sept. 2007 (10 plots)                      |
| <i>Poa alsodes</i>             | <i>E. alsodes</i>                 | 7 days drying oven (60 °C)      | Sept. 2007 (8 plots)/April 2008 (10 plots) |
| <i>Poa sylvestris</i>          | <i>E. PsyTG-1</i>                 | 7 days drying oven (60 °C)      | Sept. 2007 (8 plots)/April 2008 (10 plots) |

1979  
1980  
1981  
1982  
1983  
1984  
1985  
1986  
1987  
1988  
1989  
1990  
1991  
1992  
1993  
1994  
1995  
1996  
1997  
1998  
1999  
2000  
2001  
2002  
2003  
2004  
2005  
2006  
2007  
2008  
2009  
2010  
2011  
2012  
2013  
2014  
2015  
2016  
2017  
2018  
2019  
2020  
2021  
2022  
2023  
2024

**Table 2** Summary of focal life history traits

| Host Species                   | Observed max age (years) | 99th percentile max age (years) | Generation time (years) | $R_0$ | Longevity (years) | Seed length (mm.) | Imperfect transmission rate (%) | Stromata observed of indiv. per species) |
|--------------------------------|--------------------------|---------------------------------|-------------------------|-------|-------------------|-------------------|---------------------------------|--|
| <i>Agrostis perennans</i>      | 11                       | 7                               | 7.6                     | 0.58  | 6.4               | 1.75              | 69.8                            | 0.0                                      |
| <i>Elymus villosus</i>         | 14                       | 14                              | 20.7                    | 0.35  | 9.8               | 7.25              | 100                             | 4.6                                      |
| <i>Elymus virginicus</i>       | 14                       | 14                              | 13.4                    | 0.25  | 12.5              | 8                 | 100                             | 0.6                                      |
| <i>Festuca subverticillata</i> | 9                        | 6                               | 6.6                     | 0.28  | 4.3               | 3.75              | 42.7                            | 0.0                                      |
| <i>Lolium arundinaceum</i>     | 12*                      | 12*                             | 27.4                    | 0.08  | 21.3              | 7                 | 100                             | 0.0                                      |
| <i>Poa alsodes</i>             | 8                        | 6                               | 9.2                     | 0.003 | 2.6               | 3.45              | 99.9                            | 0.0                                      |
| <i>Poa syvestris</i>           | 12                       | 6                               | 8.0                     | 0.14  | 3.2               | 2.6               | 16.6                            | 0.1                                      |

\*Censuses for *L. arundinaceum* plots stopped after year 12 of the experiment.

2025  
2026  
2027  
2028  
2029  
2030  
2031  
2032  
2033  
2034  
2035  
2036  
2037  
2038  
2039  
2040  
2041  
2042  
2043  
2044  
2045  
2046  
2047  
2048  
2049  
2050  
2051  
2052  
2053  
2054  
2055  
2056  
2057  
2058  
2059  
2060  
2061  
2062  
2063  
2064  
2065  
2066  
2067  
2068  
2069  
2070

**Table 3** Summary of host-endophyte drought sensitivities

| Host Species                   | Effect on CV( $\lambda$ ) | Effect on Mean( $\lambda$ ) | $\frac{\Delta\lambda^-}{\Delta SPEI_3}$ | $\frac{\Delta\lambda^+}{\Delta SPEI_3}$ | 3 month S- to S+ ratio | $\frac{\Delta\lambda^-}{\Delta SPEI_{12}}$ | $\frac{\Delta\lambda^+}{\Delta SPEI_{12}}$ | 12 month S- to S+ ratio |
|--------------------------------|---------------------------|-----------------------------|---|---|------------------------|--|--|-------------------------|
| <i>Agrostis perennans</i>      | -0.0264                   | 0.0441                      | 0.03                                    | -0.04                                   | 0.85                   | 0.11                                       | -0.06                                      | 1.82                    |
| <i>Elymus villosus</i>         | 0.0003                    | 0.0509                      | -0.03                                   | 0.01                                    | 1.95                   | 0.03                                       | 0.04                                       | 0.70                    |
| <i>Elymus virginicus</i>       | 0.0120                    | 0.0578                      | 0.07                                    | 0.05                                    | 1.50                   | 0.10                                       | 0.07                                       | 1.42                    |
| <i>Festuca subverticillata</i> | -0.0622                   | 0.1639                      | 0.02                                    | 0.02                                    | 1.01                   | -0.13                                      | -0.09                                      | 1.43                    |
| <i>Lolium arundinaceum</i>     | -0.0118                   | 0.1022                      | -0.01                                   | 0.01                                    | 1.32                   | 0.03                                       | -0.03                                      | 1.02                    |
| <i>Poa alsodes</i>             | -0.1179                   | 0.1282                      | 0.10                                    | 0.14                                    | 0.71                   | 0.11                                       | 0.14                                       | 0.73                    |
| <i>Poa sylvestris</i>          | -0.0298                   | -0.0085                     | 0.07                                    | 0.16                                    | 0.44                   | 0.05                                       | 0.10                                       | 0.55                    |

2071 **References**

- 2072 [1] Seneviratne, S. *et al.* *Changes in climate extremes and their impacts on the*  
2073 *natural physical environment* (Cambridge University Press, 2012).
- 2075 [2] IPCC. Climate change 2021: The physical science basis (2021). URL <https://www.ipcc.ch/report/ar6/wg1/>.
- 2076 [3] Lewontin, R. C. & Cohen, D. On Population Growth in a Randomly Varying Envi-  
2077 *ronment. Proceedings of the National Academy of Sciences* **62**, 1056–1060 (1969).  
2078 URL <https://www.pnas.org/content/62/4/1056>. Publisher: National Academy of  
2079 Sciences Section: Biological Sciences: Zoology.
- 2080 [4] Tuljapurkar, S. D. Population dynamics in variable environments. III. Evolution-  
2081 *ary dynamics of r-selection. Theoretical Population Biology* **21**, 141–165 (1982).  
2082 URL <http://www.sciencedirect.com/science/article/pii/0040580982900107>.
- 2083 [5] Cohen, J. E. Comparative statics and stochastic dynamics of age-structured  
2084 populations. *Theoretical population biology* **16**, 159–171 (1979).
- 2085 [6] Tuljapurkar, S. *Population dynamics in variable environments* Vol. 85 (Springer  
2086 Science & Business Media, 2013).
- 2087 [7] Pfister, C. A. Patterns of variance in stage-structured populations: evolutionary  
2088 predictions and ecological implications. *Proceedings of the National Academy of  
2089 Sciences* **95**, 213–218 (1998).
- 2090 [8] Morris, W. F. *et al.* Longevity can buffer plant and animal populations against  
2091 changing climatic variability. *Ecology* **89**, 19–25 (2008).
- 2092 [9] Compagnoni, A. *et al.* The effect of demographic correlations on the stochastic  
2093 population dynamics of perennial plants. *Ecological Monographs* **86**, 480–494  
2094 (2016).
- 2095 [10] Ellis, M. M. & Crone, E. E. The role of transient dynamics in stochastic  
2096 population growth for nine perennial plants. *Ecology* **94**, 1681–1686 (2013).
- 2097 [11] Rodríguez-Caro, R. C. *et al.* The limits of demographic buffering in coping with  
2098 environmental variation. *Oikos* **130**, 1346–1358 (2021).
- 2099 [12] Tuljapurkar, S. & Orzack, S. H. Population dynamics in variable environments i.  
2100 long-run growth rates and extinction. *Theoretical Population Biology* **18**, 314–342  
2101 (1980).
- 2102 [13] Fieberg, J. & Ellner, S. P. Stochastic matrix models for conservation and  
2103 management: a comparative review of methods. *Ecology letters* **4**, 244–266 (2001).
- 2104
- 2105
- 2106
- 2107
- 2108
- 2109
- 2110
- 2111
- 2112
- 2113
- 2114
- 2115
- 2116

- [14] Menges, E. S. Applications of population viability analyses in plant conservation. *Ecological Bulletins* 73–84 (2000). 2117  
2118  
2119
- [15] Kuparinen, A., Boit, A., Valdovinos, F. S., Lassaux, H. & Martinez, N. D. Fishing-induced life-history changes degrade and destabilize harvested ecosystems. *Scientific reports* **6**, 22245 (2016). 2120  
2121  
2122
- [16] Hilde, C. H. *et al.* The Demographic Buffering Hypothesis: Evidence and Challenges. *Trends in Ecology & Evolution* **0** (2020). URL [https://www.cell.com/trends/ecology-evolution/abstract/S0169-5347\(20\)30050-1](https://www.cell.com/trends/ecology-evolution/abstract/S0169-5347(20)30050-1). Publisher: Elsevier. 2123  
2124  
2125  
2126
- [17] Rodriguez, R., White Jr, J., Arnold, A. E. & Redman, a. R. a. Fungal endophytes: diversity and functional roles. *New phytologist* **182**, 314–330 (2009). 2127  
2128  
2129
- [18] McFall-Ngai, M. *et al.* Animals in a bacterial world, a new imperative for the life sciences. *Proceedings of the National Academy of Sciences* **110**, 3229–3236 (2013). 2130  
2131  
2132  
2133
- [19] Funkhouser, L. J. & Bordenstein, S. R. Mom knows best: the universality of maternal microbial transmission. *PLoS biology* **11**, e1001631 (2013). 2134  
2135  
2136
- [20] Fine, P. E. Vectors and vertical transmission: an epidemiologic perspective. *Annals of the New York Academy of Sciences* **266**, 173–194 (1975). 2137  
2138  
2139
- [21] Russell, J. A. & Moran, N. A. Costs and benefits of symbiont infection in aphids: variation among symbionts and across temperatures. *Proceedings of the Royal Society B: Biological Sciences* **273**, 603–610 (2006). 2140  
2141  
2142  
2143
- [22] Kivlin, S. N., Emery, S. M. & Rudgers, J. A. Fungal symbionts alter plant responses to global change. *American Journal of Botany* **100**, 1445–1457 (2013). 2144  
2145
- [23] Dunbar, H. E., Wilson, A. C. C., Ferguson, N. R. & Moran, N. A. Aphid thermal tolerance is governed by a point mutation in bacterial symbionts. *PLoS biology* **5**, e96 (2007). 2146  
2147  
2148  
2149
- [24] Reyna, R., Cooke, P., Grum, D., Cook, D. & Creamer, R. Detection and localization of the endophyte undifilum oxytropis in locoweed tissues. *Botany* **90**, 1229–1236 (2012). 2150  
2151  
2152  
2153
- [25] Saikkinen, K., Gundel, P. E. & Helander, M. Chemical ecology mediated by fungal endophytes in grasses. *Journal of chemical ecology* **39**, 962–968 (2013). 2154  
2155  
2156
- [26] Neyaz, M., Gardner, D. R., Creamer, R. & Cook, D. Localization of the swainsonine-producing chaetothyriales symbiont in the seed and shoot apical meristem in its host ipomoea carnea. *Microorganisms* **10**, 545 (2022). 2157  
2158  
2159  
2160
- [27] Chamberlain, S. A., Bronstein, J. L. & Rudgers, J. A. How context dependent are species interactions? *Ecology letters* **17**, 881–890 (2014). 2161  
2162

- 2163 [28] Jordano, P. Spatial and temporal variation in the avian-frugivore assemblage of  
2164 prunus mahaleb: patterns and consequences. *Oikos* **479–491** (1994).
- 2165
- 2166 [29] Leuchtmann, A. Systematics, distribution, and host specificity of grass endo-  
2167 phytes. *Natural toxins* **1**, 150–162 (1992).
- 2168
- 2169 [30] Cheplick, G. P., Faeth, S. & Faeth, S. H. *Ecology and evolution of the grass-*  
2170 *endophyte symbiosis* (OUP USA, 2009).
- 2171
- 2172 [31] Brem, D. & Leuchtmann, A. Epichloë grass endophytes increase herbivore resis-  
2173 tance in the woodland grass *brachypodium sylvaticum*. *Oecologia* **126**, 522–530  
2174 (2001).
- 2175
- 2176 [32] Decunta, F. A., Pérez, L. I., Malinowski, D. P., Molina-Montenegro, M. A. &  
2177 Gundel, P. E. A systematic review on the effects of epichloë fungal endophytes  
2178 on drought tolerance in cool-season grasses. *Frontiers in plant science* **12**, 644731  
2179 (2021).
- 2180
- 2181 [33] Bacon, C. W. & White, J. F. in *Stains, media, and procedures for analyzing*  
2182 *endophytes* 47–56 (CRC Press, 2018).
- 2183
- 2184 [34] Rudgers, J. A. & Swafford, A. L. Benefits of a fungal endophyte in *elymus*  
2185 *virginicus* decline under drought stress. *Basic and Applied Ecology* **10**, 43–51  
2186 (2009).
- 2187
- 2188 [35] Bultman, T. L., White Jr, J. F., Bowdish, T. I., Welch, A. M. & Johnston, J.  
2189 Mutualistic transfer of epichloë spermatia by phorbia flies. *Mycologia* **87**, 182–189  
2190 (1995).
- 2191
- 2192 [36] Stan Development Team. RStan: the R interface to Stan (2022). URL <https://mc-stan.org/>. R package version 2.21.7.
- 2193
- 2194 [37] Elderd, B. D. & Miller, T. E. Quantifying demographic uncertainty: Bayesian  
2195 methods for integral projection models. *Ecological Monographs* **86**, 125–144  
2196 (2016).
- 2197
- 2198 [38] Gabry, J., Simpson, D., Vehtari, A., Betancourt, M. & Gelman, A. Visualization  
2199 in bayesian workflow. *Journal of the Royal Statistical Society Series A: Statistics*  
2200 in Society **182**, 389–402 (2019).
- 2201
- 2202 [39] Brooks, S. P. & Gelman, A. General methods for monitoring convergence of  
2203 iterative simulations. *Journal of computational and graphical statistics* **7**, 434–455  
2204 (1998).
- 2205
- 2206 [40] Gelman, A. & Hill, J. *Data analysis using regression and multilevel/hierarchical*  
2207 *models* (Cambridge university press, 2006).
- 2208

- [41] Williams, J. L., Miller, T. E. & Ellner, S. P. Avoiding unintentional eviction from integral projection models. *Ecology* **93**, 2008–2014 (2012). 2209  
2210  
2211
- [42] Jones, O. R. *et al.* Rcompadre and rage—two r packages to facilitate the use of the compadre and comadre databases and calculation of life-history traits from matrix population models. *Methods in Ecology and Evolution* **13**, 770–781 (2022). 2212  
2213  
2214  
2215  
2216  
2217  
2218  
2219
- [43]
- [44] Bürkner, P.-C. brms: An R package for Bayesian multilevel models using Stan. *Journal of Statistical Software* **80**, 1–28 (2017). 2220  
2221  
2222
- [45] Zanne, A. E. *et al.* Three keys to the radiation of angiosperms into freezing environments. *Nature* **506**, 89–92 (2014). 2223  
2224  
2225  
2226
- [46] Leuchtmann, A., Bacon, C. W., Schardl, C. L., White Jr, J. F. & Tadych, M. Nomenclatural realignment of neotyphodium species with genus epichloë. *Mycologia* **106**, 202–215 (2014). 2227  
2228  
2229  
2230
- [47] Metcalf, C. J. E. *et al.* Statistical modelling of annual variation for inference on stochastic population dynamics using integral projection models. *Methods in Ecology and Evolution* **6**, 1007–1017 (2015). 2231  
2232  
2233  
2234  
2235
- [48] Caswell, H. Matrix population models: Construction, analysis, and interpretation. 2nd edn sinauer associates. Inc., Sunderland, MA (2001). 2236  
2237  
2238  
2239
- [49] Rees, M. & Ellner, S. P. Integral projection models for populations in temporally varying environments. *Ecological Monographs* **79**, 575–594 (2009). 2240  
2241  
2242
- [50] Vicente-Serrano, S. M., Beguería, S. & López-Moreno, J. I. A multiscalar drought index sensitive to global warming: the standardized precipitation evapotranspiration index. *Journal of climate* **23**, 1696–1718 (2010). 2243  
2244  
2245  
2246
- [51] Rudgers, J. A. & Clay, K. An invasive plant–fungal mutualism reduces arthropod diversity. *Ecology Letters* **11**, 831–840 (2008). 2247  
2248  
2249
- [52] Crawford, K. M., Land, J. M. & Rudgers, J. A. Fungal endophytes of native grasses decrease insect herbivore preference and performance. *Oecologia* **164**, 431–444 (2010). 2250  
2251  
2252  
2253  
2254
- [53] Murphy, G. I. Pattern in life history and the environment. *The American Naturalist* **102**, 391–403 (1968).
- [54] Compagnoni, A. *et al.* Herbaceous perennial plants with short generation time have stronger responses to climate anomalies than those with longer generation time. *Nature communications* **12**, 1–8 (2021).

- 2255 [55] Le Coeur, C., Yoccoz, N. G., Salguero-Gómez, R. & Vindenes, Y. Life his-  
2256 tory adaptations to fluctuating environments: Combined effects of demographic  
2257 buffering and lability. *Ecology Letters* **25**, 2107–2119 (2022).
- 2258
- 2259 [56] Rees, M. Evolutionary ecology of seed dormancy and seed size. *Philosophical  
2260 Transactions of the Royal Society of London. Series B: Biological Sciences* **351**,  
2261 1299–1308 (1996).
- 2262
- 2263 [57] Moles, A. T. & Westoby, M. Seedling survival and seed size: a synthesis of the  
2264 literature. *Journal of Ecology* **92**, 372–383 (2004).
- 2265
- 2266 [58] Afkhami, M. E. & Rudgers, J. A. Symbiosis lost: imperfect vertical transmission  
2267 of fungal endophytes in grasses. *The American Naturalist* **172**, 405–416 (2008).
- 2268
- 2269 [59] Jeschke, J. M. & Kokko, H. The roles of body size and phylogeny in fast and  
2270 slow life histories. *Evolutionary Ecology* **23**, 867–878 (2009).
- 2271
- 2272 [60] Afkhami, M. E. & Strauss, S. Y. Native fungal endophytes suppress an exotic  
2273 dominant and increase plant diversity over small and large spatial scales. *Ecology*  
2274 **97**, 1159–1169 (2016).
- 2275
- 2276 [61] Smith, E., Vaughan, G., Ketchum, R., McParland, D. & Burt, J. Symbiont  
2277 community stability through severe coral bleaching in a thermally extreme lagoon.  
2278 *Scientific Reports* **7**, 2428 (2017).
- 2279
- 2280 [62] Dallas, J. W. & Warne, R. W. Captivity and animal microbiomes: potential roles  
2281 of microbiota for influencing animal conservation. *Microbial Ecology* 1–19 (2022).
- 2282
- 2283 [63] Wu, L. *et al.* Reduction of microbial diversity in grassland soil is driven by  
2284 long-term climate warming. *Nature Microbiology* **7**, 1054–1062 (2022).
- 2285
- 2286 [64] Ehrlén, J. & Morris, W. F. Predicting changes in the distribution and abundance  
2287 of species under environmental change. *Ecology letters* **18**, 303–314 (2015).
- 2288
- 2289 [65] Chamberlain, S., Hocking, D. & Anderson, B. Package ‘rnoaa’ (2022).
- 2290
- 2291
- 2292
- 2293
- 2294
- 2295
- 2296
- 2297
- 2298
- 2299
- 2300